

Helical ordering in the ground state of spin-one color superconductors as a consequence of parity violation

Tomáš Brauner*

*Institut für Theoretische Physik, Goethe-Universität,
Max-von-Laue-Straße 1, D-60438 Frankfurt am Main, Germany†*

We investigate spin-one color superconductivity of a single quark flavor using the Ginzburg–Landau theory. First we examine the classic analysis of Bailin and Love and show that by restricting to the so-called inert states, it misses the true ground state in a part of the phase diagram. This suggests the use of the more general, noninert states in particular within three-flavor quark matter where the color neutrality constraint imposes stress on the spin-one pairing and may disfavor the symmetric color-spin-locked state. In the second part of the paper we show that, in analogy to some ferromagnetic materials, lack of space-inversion symmetry leads to a new term in the Ginzburg–Landau functional, which favors a spatially nonuniform long-range ordering with a spiral structure. In color superconductors, this new parity-violating term is a tiny effect of weak-interaction physics. The modified phase diagram is determined and the corresponding ground states for all the phases constructed. At the end, we estimate the coefficient of the new term in the free energy functional, and discuss its relevance for the phenomenology of dense quark matter.

PACS numbers: 21.65.Qr, 74.20.De

Keywords: Color superconductivity, Helical ordering, Ginzburg–Landau theory

I. INTRODUCTION

It has been known for a long time that certain magnetic materials (e.g. MnSi and $\text{Fe}_x\text{Co}_{1-x}\text{Si}$) exhibit spatially nonuniform ordering with a long-wavelength helical structure. This phenomenon was first explained by Dzyaloshinsky [1] and Moriya [2] fifty years ago. They pointed out that the lack of inversion symmetry of the underlying crystal lattice allows a new term in the Ginzburg–Landau free energy functional (hereafter referred to as the DM term), which makes the uniform ferromagnetic ground state unstable with respect to the formation of the helical spin density wave. A similar effect also occurs in antiferromagnets [3]. Microscopically, the DM term results from the spin-orbit coupling. The theory of helical magnetism was developed to its present form two decades after the original discovery [4, 5], and is still a subject of intensive research in the condensed-matter-physics community [6, 7, 8].

In the present paper we show that this phenomenon has an analogy in a vastly different branch of physics, namely in strongly-interacting cold dense quark matter, which exhibits color superconductivity (see [9] for a recent review). The necessary ingredients for the helical ordering to take place are a vector (spin) order parameter and lack of space-inversion symmetry. We will therefore concentrate on spin-one color superconductivity. We will show that in this case, the parity-violating DM term is induced by weak interactions.

Due to the exchange of gluons, the quark Cooper

pairs are formed predominantly in the spin-zero color-antitriplet channel. At very high baryon density where the quark masses can be neglected, the cold three-flavor quark matter is known to be in the so-called color-flavor-locked phase. However, at densities corresponding to the neutron star cores the large value of the strange quark mass as well as the charge neutrality constraint induce a mismatch of the Fermi levels of different quark flavors, and thus impose stress on the cross-flavor pairing. Other forms of pairing are then likely to occur. Depending on the size of the Fermi surface mismatch, quarks of two flavors and two colors may combine in the so-called 2SC phase. When the mismatch is too large, only quarks of the same flavor can pair and the spin-one pairing then remains the only possibility [9].

Originally spin-one color superconductivity was suggested and studied as a mechanism for pairing of quarks of a single flavor [10, 11, 12, 13], or a single color [14], left over from the 2SC pairing. The classification and physical properties of several spin-one color-superconducting phases were worked out in a series of papers by Schmitt *et al.* [15, 16, 17, 18, 19]. Possible impacts of spin-one color superconductivity on the phenomenology of compact stars were studied in Refs. [20, 21, 22, 23, 24, 25, 26, 27]. A different approach to spin-one color superconductivity, based on the Schwinger–Dyson equations, was investigated in [28].

The weak-coupling quantum chromodynamics (QCD) calculations at asymptotically high density show that the ground state of the single-flavor quark matter is the color-spin-locked (CSL) phase. However, when spin-one color superconductivity is considered within three-flavor quark matter (e.g. as a complement to the primary 2SC pairing), the requirement of overall color neutrality may favor other patterns of spin-one pairing [29]. We will therefore in the main body of this paper perform a phenomenologi-

†On leave from Department of Theoretical Physics, Nuclear Physics Institute ASCR, CZ-25068 Řež, Czech Republic

*Electronic address: brauner@ujf.cas.cz

cal analysis based on the Ginzburg–Landau (GL) theory, treating the coefficients in the free energy as unknown parameters.

The plan of the paper is as follows. We start in Sec. II by investigating the possible forms that the order parameter in a single-flavor spin-one color superconductor may take. Such a classification was already done by Schmitt [19] for the sake of weak-coupling QCD calculations. However, while in QCD the order parameter is provided by a nontrivial function of momentum near the Fermi surface—the gap function, in the GL description we deal with a single (local) order parameter. This greatly simplifies the analysis, allowing us to carry out a complete classification of the possible symmetry-breaking patterns.

In Sec. III we review the GL theory for spin-one color superconductivity without the parity-violating DM term. This was already developed by Bailin and Love more than twenty years ago [10]. Nevertheless, they restricted their attention to the so-called inert states, proposing that one with the lowest free energy for the ground state. Here we derive a set of inequalities between the independent quartic terms in the GL functional which allow us to determine the unique absolute minimum of the free energy. We thus show that there is a sector in the phase diagram where the true ground state is actually noninert.

In Sec. IV we finally introduce the parity-violating DM term into the GL free energy functional. Based on Ref. [8] we first work out the (slightly generalized) theory of the helical spin density wave in the ferromagnets. With all the necessary formalism ready, we then construct the corresponding helical states for the spin-one color-superconducting phases, and determine the modified phase diagram.

In Sec. V we demonstrate how the DM term arises from weak-interaction physics. We estimate the corresponding coefficient in the weak-coupling limit. In Sec. VI we then discuss the possible relevance of this effect for the phenomenology of dense quark matter. In Sec. VII we summarize and conclude.

It should be noted that while some calculations such as the derivation of the Ginzburg–Landau free energy in the high-density, weak-coupling approximation are standard and the details may thus certainly be omitted, the algebraic analysis presented in Sections II, III, and IV is particular to spin-one color superconductivity. Even though all derivations are based on elementary linear algebra and require no lengthy computations, we choose to provide most details since they cannot be found elsewhere. For reader’s convenience, we formulate some purely mathematical auxiliary material in the form of simple theorems and defer the full proofs to the appendices.

II. CLASSIFICATION OF ORDER PARAMETERS

In this section we will investigate the possible symmetry-breaking patterns in a single-flavor spin-one color superconductor. The order parameter transforms as an antitriplet under $SU(3)$ color transformations, as a vector under spatial $SO(3)$ rotations, and carries charge of the baryon number $U(1)$ group. It can be represented by a complex 3×3 matrix, Δ_{ai} , which transforms as [19]

$$\Delta \rightarrow U \Delta R, \quad (1)$$

where $U \in SU(3) \times U(1) \equiv U(3)_L$ and $R \in SO(3)_R$. The indices L and R denote the “left” and “right” symmetry groups, acting on the order parameter. This symmetry structure is similar to that of the superfluid Helium 3 [30]. However, since the symmetry group of the spin-one color superconductors is larger than that of the superfluid Helium [which has another $SO(3)$ instead of the $SU(3)$], the classification will be somewhat simpler in the present case.

In the following it will be helpful to consider also transformations from the “diagonal” subgroup, $SO(3)_V$,

$$\Delta \rightarrow R^T \Delta R. \quad (2)$$

The classification of the possible inequivalent forms of the order parameter will be based on the following two claims which are proved in Appendix A.

Theorem 1 *By a suitable symmetry transformation, the order parameter can always be brought in the form,*

$$\Delta = \begin{pmatrix} \Delta_1 & ia_3 & -ia_2 \\ -ia_3 & \Delta_2 & ia_1 \\ ia_2 & -ia_1 & \Delta_3 \end{pmatrix} \quad (3)$$

(with real parameters Δ_i, a_i), being a Hermitian, positive-semidefinite matrix.

Theorem 2 *Let the order parameter have the form (3) and $U \in U(3)_L$, $R \in SO(3)_V$. Then*

$$UR^T \Delta R = \Delta \quad (4)$$

if and only if $U \Delta = \Delta$ and $R^T \Delta R = \Delta$.

Eq. (3) represents the simplest form to which the order parameter can in general be cast. As could have been expected, it contains six independent parameters: A complex 3×3 matrix has altogether 18 real parameters, 12 of which can be fixed by a transformation from the 12-parametric symmetry group, $G \equiv U(3)_L \times SO(3)_R$. We will classify all special forms of the order parameter which leave some *continuous* subgroup of G unbroken. The analysis is greatly simplified by Theorem 2 which ensures that one can separately investigate invariance under left unitary transformations from $U(3)_L$, and diagonal orthogonal rotations from $SO(3)_V$. [The transformed order

parameter (1) can always be written as on the left-hand side of Eq. (4) by the substitution $U \rightarrow UR^T$, which is just another matrix from $U(3)_L$.] There is no nontrivial unbroken combination of transformations from the two groups. Therefore, we just need to classify the unbroken subgroups of $U(3)_L$ and $SO(3)_V$.

As follows from the polar decomposition, Theorem 7, given in Appendix A, $U(3)_L$ has a nontrivial unbroken subgroup if and only if the matrix Δ has zero modes. Specifically, the unbroken subgroup will be $U(n)_L$ where n is the number of zero modes of Δ .

The possible unbroken subgroups of $SO(3)_V$ may be found by elementary geometry. The Hermitian order parameter Δ is written as a sum of its real symmetric and imaginary antisymmetric parts, $\Delta = S + iA$. These obviously transform separately under the diagonal subgroup $SO(3)_V$. Moreover, the antisymmetric part is parameterized as $A_{ij} = \epsilon_{ijk}a_k$ so that the three components a_i transform as a vector, \vec{a} . The (real) symmetric matrix S may be viewed as defining a quadratic surface with principal values $\Delta_1, \Delta_2, \Delta_3$. Apparently, it possesses the same symmetry as A if and only if this quadratic surface is axially symmetric, with the axis given by \vec{a} . This constrains S to be of the form

$$S_{ij} = \alpha\delta_{ij} + \beta a_i a_j,$$

or equivalently a linear combination of identity and the projector to the plane perpendicular to \vec{a} , $\mathcal{P}_{ij} = \delta_{ij} - \frac{a_i a_j}{\|\vec{a}\|^2}$. Since S is actually diagonal, obviously at most one component of \vec{a} may be nonzero (or $\beta = 0$) in order to preserve a continuous subgroup of $SO(3)_V$.

By combining the conditions for invariance under the left unitary and the diagonal orthogonal transformations, one arrives at the classification summarized in Fig. 1. The logic of the table is simple. First four rows display phases with nonzero \vec{a} in order of increasing unbroken symmetry. The next two rows show the CSL and polar phases, whose order parameter is diagonal. Then come the phases N_1, N_2 that completely break the $SO(3)_V$. These cannot be easily cast in the form (3) and we thus display them in such a way as to manifest the number of zero modes. Finally, the axial and planar states, showed under the double line, are just special cases of the oblate and cylindrical ones, already included in the table. They are distinguished by an unbroken discrete symmetry, generated by the permutation matrix

$$P = \begin{pmatrix} 0 & 1 & 0 \\ 1 & 0 & 0 \\ 0 & 0 & -1 \end{pmatrix},$$

that is, a rotation by π about the line $x = y, z = 0$. We do not have the ambition to extend the above analysis to unbroken *discrete* symmetries. These two special cases are mentioned explicitly because they will later turn out to occupy a part of the phase diagram.

Four of the indicated phases are “inert”, i.e., their order parameter is fixed up to a symmetry transformation

and an overall normalization. These are the A, CSL, planar, and polar phases. Note that some of the states that are distinct according to Ref. [19], are classified as equivalent here. This is because (as already remarked above) we treat the matrix elements of Δ as pure numbers, not functions of momentum.

A remark about the nomenclature is in order here. The names of the four inert phases are standard in literature on spin-one color superconductivity. The terms “oblate” [30] and “ ε ” [31] have been taken over from literature on superfluid Helium 3. The remaining four names are new. The “N” states are labeled by the degeneracy of the zero eigenvalue of Δ . In the “cylindrical” phase, the quadratic form S defines a cylinder with the vector \vec{a} pointing along its axis. Finally, the “axial” state may be thought of as deformed CSL with just axial symmetry. As we will see in Sec. IV B 3, this exactly happens to the CSL phase upon switching on the DM term [49].

III. GINZBURG–LANDAU THEORY WITHOUT DM TERM

After working out the classification of all inequivalent forms of the order parameter, we now investigate using the Ginzburg–Landau theory, which of the states is actually energetically preferred. Our analysis will be similar to that of Baym and Iida for spin-zero color superconductivity [32]. So far, we do not include the DM term. In the following one should always keep in mind that the GL theory is strictly speaking only valid near the critical temperature. For the sake of brevity, we often use the term “ground state” where we mean the state minimizing the free energy, i.e., thermodynamic equilibrium. It is only in Sec. VI that we make some speculations concerning the physics far from the critical point, at low temperatures.

It will sometimes be convenient to use a different notation for the order parameter, in particular to treat the matrix Δ_{ai} as a collection of three complex vectors, $\vec{\phi}_a$, one for each anticolor a . The GL free energy density up to fourth order in Δ then reads

$$\mathcal{F}[\vec{\phi}_a] = a_1 \nabla_i \vec{\phi}_a^\dagger \cdot \nabla_i \vec{\phi}_a + a_2 (\vec{\nabla} \cdot \vec{\phi}_a^\dagger)(\vec{\nabla} \cdot \vec{\phi}_a) + b \vec{\phi}_a^\dagger \cdot \vec{\phi}_a + d_1 \mathcal{A} + d_2 \mathcal{B} + d_3 \mathcal{C}. \quad (5)$$

For the time being, the parameters $a_1, a_2, b, d_1, d_2, d_3$ are treated as free, constrained only by the requirement of boundedness of the free energy from below. There are three independent quartic G-invariant terms that we denote as \mathcal{A}, \mathcal{B} , and \mathcal{C} . Their explicit forms in both notations for the order parameter are summarized in Fig. 2.

order parameter	unbroken symmetry	name	name according to [19]
$\begin{pmatrix} \Delta_1 & +ia & 0 \\ -ia & \Delta_1 & 0 \\ 0 & 0 & \Delta_2 \end{pmatrix}$	$\text{SO}(2)_V$	oblate	—
$\begin{pmatrix} \Delta & +ia & 0 \\ -ia & \Delta & 0 \\ 0 & 0 & 0 \end{pmatrix}$	$\text{SO}(2)_V \times \text{U}(1)_L$	cylindrical	—
$\begin{pmatrix} \Delta_1 & +i\Delta_1 & 0 \\ -i\Delta_1 & \Delta_1 & 0 \\ 0 & 0 & \Delta_2 \end{pmatrix}$	$\text{SO}(2)_V \times \text{U}(1)_L$	ϵ	P_7, P_8
$\begin{pmatrix} 1 & +i & 0 \\ -i & 1 & 0 \\ 0 & 0 & 0 \end{pmatrix}$	$\text{SU}(2)_L \times \text{SO}(2)_V \times \text{U}(1)_L$	A	A, P_3, P_5
$\begin{pmatrix} 1 & 0 & 0 \\ 0 & 1 & 0 \\ 0 & 0 & 1 \end{pmatrix}$	$\text{SO}(3)_V$	CSL	CSL
$\begin{pmatrix} 0 & 0 & 0 \\ 0 & 0 & 0 \\ 0 & 0 & 1 \end{pmatrix}$	$\text{SU}(2)_L \times \text{SO}(2)_R \times \text{U}(1)_L$	polar	polar, P_2, P_6
$\begin{pmatrix} 0 & 0 & 0 \\ z_1 & z_2 & z_3 \\ z_4 & z_5 & z_6 \end{pmatrix}$	$\text{U}(1)_L$	N_1	P_4
$\begin{pmatrix} 0 & 0 & 0 \\ 0 & 0 & 0 \\ z_1 & z_2 & z_3 \end{pmatrix}$	$\text{SU}(2)_L \times \text{U}(1)_L$	N_2	P_1
$\begin{pmatrix} \Delta_1 & 0 & 0 \\ 0 & \Delta_1 & 0 \\ 0 & 0 & \Delta_2 \end{pmatrix}$	$\text{SO}(2)_V$	axial	—
$\begin{pmatrix} 1 & 0 & 0 \\ 0 & 1 & 0 \\ 0 & 0 & 0 \end{pmatrix}$	$\text{SO}(2)_V \times \text{U}(1)_L$	planar	planar

FIG. 1: Classification of all order parameters that leave some continuous subgroup of G unbroken. The parameters z_i are complex, while all other parameters are real, in accordance with Eq. (3). For convenience, we explicitly distinguish the $\text{SO}(2)$ group of real rotations from the $\text{U}(1)$ group of phase transformations, even though the two are actually isomorphic. The first eight rows represent all possible phases distinguished by the unbroken continuous symmetry. The last two rows—the axial and planar states—are merely special cases of the oblate and cylindrical ones which have an additional discrete symmetry.

name	vector expression	matrix expression
\mathcal{A}	$(\vec{\phi}_a^\dagger \cdot \vec{\phi}_a)^2$	$[\text{Tr}(\Delta\Delta^\dagger)]^2$
\mathcal{B}	$ \vec{\phi}_a^\dagger \cdot \vec{\phi}_b ^2$	$\text{Tr}(\Delta\Delta^\dagger\Delta\Delta^\dagger)$
\mathcal{C}	$ \vec{\phi}_a \cdot \vec{\phi}_b ^2$	$\text{Tr}[\Delta\Delta^T(\Delta\Delta^T)^\dagger]$

FIG. 2: Independent quartic invariants and their expression using the matrix Δ as well as the complex vectors $\vec{\phi}_a$.

A. Ground state

Since the gradient part of the free energy is required to be bounded from below, the ground state is apparently a uniform field configuration that minimizes the static part of Eq. (5). As usual, the “mass term” b changes

sign at the critical temperature. In the following we will assume that it is negative (i.e., we are in the superfluid phase) so that the free energy has a nontrivial minimum. We will use the invariant \mathcal{A} to measure the size of the condensate; actually, it is a squared norm of Δ in the sense that will be specified later. The values of the other invariants \mathcal{B}, \mathcal{C} then measure the orientation of the order parameter in the color and spin space, and we will draw the phase diagram in the two-dimensional space of the parameters d_2, d_3 .

Trying to determine the ground state by a direct solution of the gap equation would be just hopeless. First, the gap equation is a coupled set of equations for the six independent parameters in Δ . Second, even if we somehow managed to solve it, we could at best show

that the solution is a local minimum of the free energy. Instead, we derive a set of inequalities between the invariants $\mathcal{A}, \mathcal{B}, \mathcal{C}$ that allow us to uniquely determine the absolute minimum of the free energy. We again formulate these inequalities as simple theorems whose proof is given in detail in Appendix B. (It is understood that all the following claims about the order parameter hold up to a symmetry transformation.)

Theorem 3 *The invariants \mathcal{A}, \mathcal{B} satisfy the following inequalities,*

$$\frac{1}{3}\mathcal{A} \leq \mathcal{B} \leq \mathcal{A}. \quad (6)$$

The first inequality is saturated (i.e., an equality holds) if and only if the order parameter is of the CSL type. The second inequality is saturated if and only if the matrix Δ has rank one.

Theorem 4 *The invariants \mathcal{B}, \mathcal{C} satisfy the following inequalities,*

$$0 \leq \mathcal{C} \leq \mathcal{B}. \quad (7)$$

The first inequality is saturated if and only if the order parameter is of the A type. The second inequality is saturated if and only if the order parameter is real.

Theorem 5 *The invariants $\mathcal{A}, \mathcal{B}, \mathcal{C}$ satisfy the following inequality,*

$$\frac{2}{3}\mathcal{A} \leq \mathcal{B} + \mathcal{C}. \quad (8)$$

The inequality is saturated if and only if the order parameter is of the oblate type with $\Delta_2 = \sqrt{\Delta_1^2 + a^2}$.

Theorem 6 *Let $\mathcal{C} \leq \frac{1}{9}\mathcal{A}$. Then the invariants $\mathcal{A}, \mathcal{B}, \mathcal{C}$ satisfy the following inequality,*

$$\sqrt{\mathcal{A}} \leq \sqrt{\mathcal{C}} + \sqrt{\mathcal{B} - \mathcal{C}}. \quad (9)$$

The inequality is saturated if and only if the order parameter is of the ε type.

With this set of inequalities at hand, it is straightforward to determine the phase diagram in the (d_2, d_3) plane. We do so by finding a lower bound on the free energy and showing that this bound is saturated by a particular type of the order parameter. In all cases, the free energy density can be, after fixing the orientation of the condensate, written as

$$\mathcal{F} = b\sqrt{\mathcal{A}} + \bar{d}\mathcal{A},$$

where \bar{d} is an effective quartic coupling, specific for the given phase. The ground state condensate and free energy are then given by

$$\sqrt{\mathcal{A}_{\min}} = -\frac{b}{2\bar{d}}, \quad \mathcal{F}_{\min} = -\frac{b^2}{4\bar{d}}. \quad (10)$$

- $d_2 + d_3 > 0, d_2 > d_3$. Using Theorems 4 and 5, we get

$$\begin{aligned} d_2\mathcal{B} + d_3\mathcal{C} &= \frac{1}{2}(d_2 + d_3)(\mathcal{B} + \mathcal{C}) \\ &+ \frac{1}{2}(d_2 - d_3)(\mathcal{B} - \mathcal{C}) \geq \frac{1}{3}(d_2 + d_3)\mathcal{A}. \end{aligned}$$

To saturate the inequality, we should have simultaneously $\mathcal{B} + \mathcal{C} = \frac{2}{3}\mathcal{A}$ and $\mathcal{B} = \mathcal{C}$, i.e., $\mathcal{B} = \frac{1}{3}\mathcal{A}$. By Theorem 3, this is only satisfied by the CSL state. The magnitude of the condensate and minimum free energy density are given by (10) with $\bar{d}_{\text{CSL}} = d_1 + \frac{d_2 + d_3}{3}$.

- $d_2 + d_3 < 0, d_3 < 0$. In this case, Theorems 3 and 4 yield

$$d_2\mathcal{B} + d_3\mathcal{C} \geq (d_2 + d_3)\mathcal{B} \geq (d_2 + d_3)\mathcal{A}.$$

The order parameter that saturates this bound should be real and have rank one, which is precisely the polar phase, with condensate and free energy determined by $\bar{d}_{\text{polar}} = d_1 + d_2 + d_3$.

- $d_2 < 0, d_3 > 0$. Now we estimate the free energy using Theorems 3 and 4 as

$$d_2\mathcal{B} + d_3\mathcal{C} \geq d_2\mathcal{A}.$$

The ground state is the A phase. The effective quartic coupling in this case reads $\bar{d}_A = d_1 + d_2$.

- $d_3 > d_2 > 0$. This case is subtle; it is here that none of the inert phases provides the absolute minimum of the free energy. Let us assume that $\mathcal{C} \leq \frac{1}{9}\mathcal{A}$. We then use Theorem 6 and the Cauchy inequality (B1) with $u_1 = \sqrt{d_2(\mathcal{B} - \mathcal{C})}, u_2 = \sqrt{(d_2 + d_3)\mathcal{C}}, v_1 = 1/\sqrt{d_2}, v_2 = 1/\sqrt{d_2 + d_3}$, to obtain

$$\begin{aligned} d_2\mathcal{B} + d_3\mathcal{C} &= d_2(\mathcal{B} - \mathcal{C}) + (d_2 + d_3)\mathcal{C} = u_1^2 + u_2^2 \geq \\ &\geq \frac{(u_1 v_1 + u_2 v_2)^2}{v_1^2 + v_2^2} = \frac{(\sqrt{\mathcal{B} - \mathcal{C}} + \sqrt{\mathcal{C}})^2}{\frac{1}{d_2} + \frac{1}{d_2 + d_3}} \geq \frac{d_2(d_2 + d_3)}{2d_2 + d_3}\mathcal{A}. \end{aligned}$$

The inequality is saturated if and only if the order parameter is of the ε type, and vectors \vec{u} and \vec{v} are collinear. This fixes the order parameter to be

$$\begin{aligned} \Delta &= \sqrt{\mathcal{A}_{\min}} \begin{pmatrix} \alpha & i\alpha & 0 \\ -i\alpha & \alpha & 0 \\ 0 & 0 & \beta \end{pmatrix}, \\ \alpha &= \frac{1}{2}\sqrt{\frac{d_2 + d_3}{2d_2 + d_3}}, \quad \beta = \sqrt{\frac{d_2}{2d_2 + d_3}}. \end{aligned} \quad (11)$$

The effective quartic coupling in this case is $\bar{d}_\varepsilon = d_1 + \frac{d_2(d_2 + d_3)}{2d_2 + d_3}$. One easily checks that the initial assumption $\mathcal{C} \leq \frac{1}{9}\mathcal{A}$ is fulfilled for considered values of d_2, d_3 .

B. Phase diagram

The calculation of the ground state for different relative values of d_2, d_3 given in the previous subsection is straightforward, but may not be entirely transparent. Therefore, we complement it here by an elegant and powerful geometric picture, first developed by Kim and Frautschi [33, 34] to analyze complicated Higgs potentials in models of grand unification. It will not only confirm our previous conclusions about the ground state, but also illuminate the nature of the inert and noninert states and the phase transitions between them.

The idea is as follows. The quartic part of the free energy can be thought of as depending on the squared norm of the condensate, \mathcal{A} , and two dimensionless quantities, $\lambda_2 = \mathcal{B}/\mathcal{A}$ and $\lambda_3 = \mathcal{C}/\mathcal{A}$. These specify the orientation of the condensate in the color and spin space. For a uniform field configuration, the free energy density thus becomes

$$\mathcal{F}_{\text{stat}} = b\sqrt{\mathcal{A}} + (d_1 + d_2\lambda_2 + d_3\lambda_3)\mathcal{A}. \quad (12)$$

The inequalities derived above show that the quantities λ_2, λ_3 cannot acquire arbitrary values. Instead, their values for all nonzero 3×3 matrices will span some domain in the (λ_2, λ_3) plane, which we will refer to as the target space, in order to distinguish it from the parameter space of d_2, d_3 . The shape of the target space is a property of the algebra of 3×3 matrices (and the symmetry group G), and is independent of the couplings d_2, d_3 .

The absolute minimum of the free energy (12) can now be found by a consecutive minimization with respect to the “angles” λ_2, λ_3 , and then the “modulus” $\sqrt{\mathcal{A}}$. But since the free energy (12) is linear in λ_2, λ_3 , the minimum will simply lie somewhere on the boundary of the target space. Which point of the boundary will realize the ground state, depends on the coefficients d_2, d_3 . For fixed values of $\mathcal{F}_{\text{stat}}$ and $\sqrt{\mathcal{A}}$, Eq. (12) defines a straight line in the (λ_2, λ_3) plane. For a too small value of $\mathcal{F}_{\text{stat}}$, this line will not intersect the target space, i.e., there is no state with the desired value of the free energy. As $\mathcal{F}_{\text{stat}}$ increases, the straight line will shift parallel until for some \mathcal{F}_{min} , it will for the first time touch the target space. The point of touch will then define the ground state.

In the case of the spin-one color superconductor, the explicit form of the target space is plotted in Fig. 3. We emphasize once again that it is the points at its boundary that will appear in the phase diagram as ground states for some particular combination of d_2, d_3 . The states that correspond to the corners of the target space therefore play a distinguished role. These are the three inert states, A, CSL, and polar. Since they are inert, they are represented by a single point in the target space. A noninert state of a particular type will occupy some nontrivial domain, depending on its number of free parameters.

Let us now be more specific about the boundary of the target space. The second inequality in Eq. (6) defines the edge connecting the “A” and “polar” corners, which

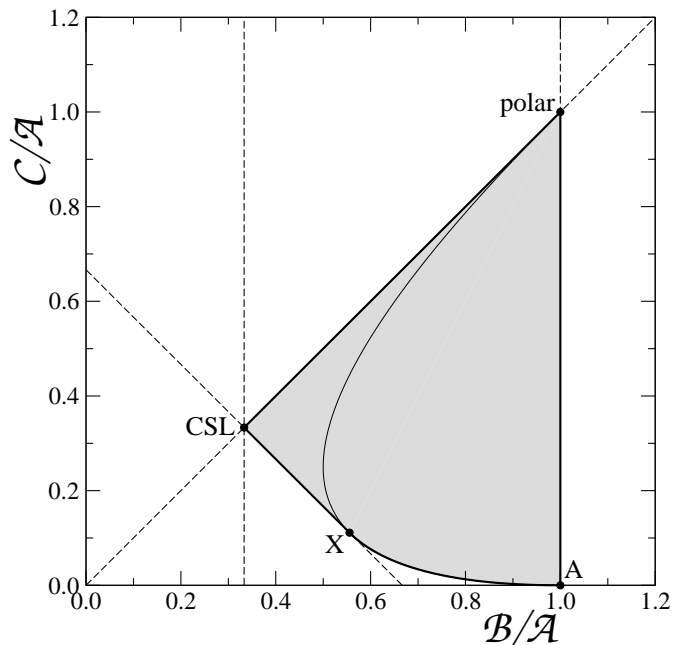


FIG. 3: Target space in the (λ_2, λ_3) plane (shaded). The various bounding curves are determined by Eqs. (6)–(9). The curve connecting the points “A”, “X”, and “polar” is defined by $\sqrt{\mathcal{C}} + \sqrt{\mathcal{B} - \mathcal{C}} = \sqrt{\mathcal{A}}$. For given d_2, d_3 the structure of the ground state is determined by that point on the boundary of the target space which minimizes the expression $d_2\lambda_2 + d_3\lambda_3$, i.e., by the nearest point of the target space when looking at it (in the plane) in the direction of the vector (d_2, d_3) .

thus involves all rank-one order parameters. The polar–CSL edge follows from the second inequality in Eq. (7) and consists of matrices Δ that can be made real by a symmetry transformation. The CSL–X edge comes from Eq. (8). It is occupied by matrices of the oblate type with $\Delta_2 = \sqrt{\Delta_1^2 + a^2}$. Finally, the curved segment X–A is a consequence of Theorem 6 and is realized by the matrices of the ε type. This completes the picture of the target space and elucidates the significance of the various inequalities.

The analysis carried out in Sec. III A yields the phase diagram, displayed in Fig. 4. Note that all phase transitions but the one between the A and ε phases are first order. This is also easily seen using the Kim–Frautschi plot of the target space (see Fig. 3). A straight segment of the boundary connecting two corners such as polar and CSL causes the ground state to change abruptly at an infinitesimal change of the slope of the straight line (12) (i.e., the ratio of d_2 and d_3). On the other hand, as we move through the ε phase towards the transition line to the A phase, the order parameter runs along the curved segment X–A until it eventually continuously enters the A phase. Moreover, we can easily check explicitly using Eq. (11) that as $d_2 \rightarrow 0+$, the ε state continuously goes to the A state.

The Kim–Frautschi plot also tells us which types of order parameters may coexist right at the first-order phase

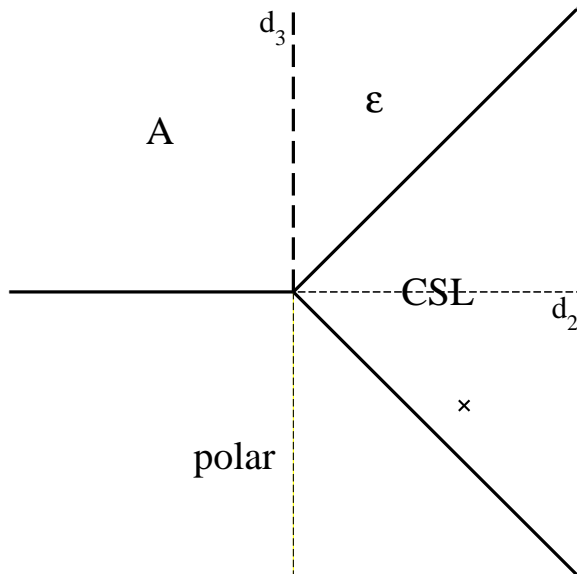


FIG. 4: Phase diagram of the spin-one color superconductor in the (d_2, d_3) plane. The solid and dashed thick lines denote first- and second-order phase transitions, respectively. The phase boundaries are defined by straight radial lines at angles $\frac{\pi}{4}, \frac{\pi}{2}, \pi, \frac{7\pi}{4}$ with respect to the d_2 axis. The cross indicates the weak-coupling prediction, see Eq. (27).

transition lines. If the segment of the boundary of the target space connecting the two competing phases were concave, we would find just these two states. However, since all the border lines corresponding to first-order phase transitions are straight, a much wider class of states can actually coexist. Without going into details we just note that special relations between d_2 and d_3 which define the phase transition lines, may bring in additional degeneracy in terms of an enhanced symmetry of the free energy [35].

Note that the phase diagram in Fig. 4 does not depend on the coefficient d_1 . The only way it affects the problem is indirectly, by the requirement of boundedness of the free energy from below. In other words, a particular value of d_1 will determine a region in the (d_2, d_3) plane which is physically allowed.

Finally, a comparison with the phase diagram calculated in Ref. [10] [and plotted in the $(d_2, d_2 + d_3)$ plane] shows that our results agree with the exception of the ε region, which was missed in [10]. The strategy used here, based on lower estimates of the free energy together with the conditions for their saturation, ensures that we have really found the absolute minimum of the free energy. Apart from the phase transition lines, it is unique up to a symmetry transformation.

IV. GINZBURG–LANDAU THEORY WITH DM TERM

We are now ready to analyze the GL theory for spin-one color superconductivity including the parity-violating DM term. However, since the construction of the helix-ordered state for some of the color-superconducting phases is a bit involved, we prefer to illustrate the idea and develop the argument on a simple toy example.

A. Toy model: Complex ferromagnet

Following closely Ref. [8], we consider the GL free energy density functional of the form [50]

$$\mathcal{F}[\vec{M}] = a_1 \nabla_i \vec{M}^\dagger \cdot \nabla_i \vec{M} + a_2 (\vec{\nabla} \cdot \vec{M}^\dagger)(\vec{\nabla} \cdot \vec{M}) + b \vec{M}^\dagger \cdot \vec{M} + c \vec{M}^\dagger \cdot (\vec{\nabla} \times \vec{M}) + d (\vec{M}^\dagger \cdot \vec{M})^2, \quad (13)$$

where the term proportional to c is the DM term. (Note that it is real up to a total derivative.) Without lack of generality we will assume that $c > 0$.

First of all we would like to stress that since the DM term will make the ground state configuration nonuniform, we are not a priori allowed to simply minimize the static part of the free energy to determine the magnitude of the order parameter \vec{M} (which we shall in this section refer to as the magnetization). Instead, we will rely on an estimate of the free energy, this time including the space dependence of the order parameter. Assuming the space has finite volume Ω with periodic boundary conditions, we expand the magnetization in Fourier modes,

$$\vec{M}(\mathbf{x}) = \sum_{\mathbf{k}} \vec{m}_{\mathbf{k}} e^{i\mathbf{k} \cdot \mathbf{x}}.$$

Using the integral form of the Cauchy inequality, we may estimate the quartic part of the free energy,

$$\int d^3 \mathbf{x} (\vec{M}^\dagger \cdot \vec{M})^2 \geq \frac{1}{\Omega} \left(\int d^3 \mathbf{x} \vec{M}^\dagger \cdot \vec{M} \right)^2 = \Omega \left(\sum_{\mathbf{k}} |\vec{m}_{\mathbf{k}}|^2 \right)^2 \equiv \Omega \mathcal{M}^2.$$

The inequality is saturated if $\vec{M}^\dagger \cdot \vec{M}$ is uniform, i.e., the magnetization has the same magnitude in the whole space.

Decomposing the Fourier mode $\vec{m}_{\mathbf{k}}$ into components parallel (“longitudinal”) and perpendicular (“transverse”) to the momentum \mathbf{k} , $\vec{m}_{\mathbf{k}\parallel}$ and $\vec{m}_{\mathbf{k}\perp}$, and the transverse component further into its real and imaginary parts, $\vec{m}_{\mathbf{k}\perp} = \vec{u}_{\mathbf{k}} + i\vec{v}_{\mathbf{k}}$, the DM contribution to the free energy becomes

$$\int d^3 \mathbf{x} \vec{M}^\dagger \cdot (\vec{\nabla} \times \vec{M}) = 2\Omega \sum_{\mathbf{k}} \mathbf{k} \cdot (\vec{u}_{\mathbf{k}} \times \vec{v}_{\mathbf{k}}).$$

Using elementary geometry, this is estimated as

$$\begin{aligned} \mathbf{k} \cdot (\vec{u}_{\mathbf{k}} \times \vec{v}_{\mathbf{k}}) &\geq -|\mathbf{k}| |\vec{u}_{\mathbf{k}} \times \vec{v}_{\mathbf{k}}| \geq \\ &\geq -|\mathbf{k}| |\vec{u}_{\mathbf{k}}| |\vec{v}_{\mathbf{k}}| \geq -|\mathbf{k}| \frac{|\vec{u}_{\mathbf{k}}|^2 + |\vec{v}_{\mathbf{k}}|^2}{2} = -\frac{1}{2} |\mathbf{k}| |\vec{m}_{\mathbf{k}\perp}|^2. \end{aligned}$$

The chain of inequalities is saturated if the real and imaginary parts of $\vec{m}_{\mathbf{k}\perp}$ have the same size, are perpendicular to each other as well as to \mathbf{k} , and together form a left-handed orthogonal system of vectors. (For $c < 0$, it would be right-handed.) Together with the gradient terms, the DM term can thus be minimized as follows,

$$\begin{aligned} &\int d^3\mathbf{x} [a_1 |\nabla_i \vec{M}|^2 + a_2 |\vec{\nabla} \cdot \vec{M}|^2 + c \vec{M}^\dagger \cdot (\vec{\nabla} \times \vec{M})] \geq \\ &\geq \Omega \sum_{\mathbf{k}} [(a_1 + a_2) |\mathbf{k}|^2 |\vec{m}_{\mathbf{k}\parallel}|^2 + (a_1 |\mathbf{k}|^2 - c |\mathbf{k}|) |\vec{m}_{\mathbf{k}\perp}|^2]. \end{aligned}$$

Stability of the system with respect to longitudinal fluctuations requires $a_1 + a_2 > 0$. The longitudinal mode $\vec{m}_{\mathbf{k}\parallel}$ therefore always increases the free energy. On the other hand, *the DM term, being linear in momentum, can outweigh the gradient term and make nonuniform, transverse field configurations energetically favorable.* The minimum free energy is achieved when only modes with $|\mathbf{k}| = |\mathbf{k}|_{\min} = c/2a_1$ are included.

Putting all the pieces together, we obtain the minimum free energy density as

$$\frac{1}{\Omega} \int d^3\mathbf{x} \mathcal{F}[\vec{M}] \geq \left(b - \frac{c^2}{4a_1} \right) \mathcal{M} + d\mathcal{M}^2. \quad (14)$$

The state minimizing the free energy will be purely transverse so that the a_2 term in Eq. (13) actually does not play any role. To specify the form of the ground state more concretely, recall that apart from being composed solely of Fourier modes with $|\mathbf{k}| = |\mathbf{k}|_{\min}$, it also ought to have a spatially uniform magnitude of magnetization. The most general state satisfying this condition has the form

$$\vec{M} = \alpha \vec{m}_{\mathbf{k}} e^{i\mathbf{k}\cdot\mathbf{x}} + \beta \vec{m}_{\mathbf{k}}^* e^{-i\mathbf{k}\cdot\mathbf{x}}, \quad (15)$$

with fixed momentum \mathbf{k} and real coefficients α, β .

Two special cases deserve particular attention. First, if α or β is zero, the ground state is a *single (complex) plane wave*. Second, if we require the order parameter to be real (which is the case of the ferromagnet as well as several of the spin-one color-superconducting phases), we arrive at

$$\vec{M} = \vec{m}_{\mathbf{k}} e^{i\mathbf{k}\cdot\mathbf{x}} + \vec{m}_{\mathbf{k}}^* e^{-i\mathbf{k}\cdot\mathbf{x}} = 2[\vec{u}_{\mathbf{k}} \cos(\mathbf{k}\cdot\mathbf{x}) - \vec{v}_{\mathbf{k}} \sin(\mathbf{k}\cdot\mathbf{x})],$$

i.e., a *real standing wave*. The magnetization evolves along a *right-handed helix* with the axis defined by the vector \mathbf{k} , and the wavelength $\lambda = 4\pi a_1/c$. This concludes the argument and reveals the nature of the ground state induced by the DM term.

Several remarks are in order here. First, for generic (nonzero) coefficients α, β , the state (15) breaks both rotational and translational invariance [51]. However, there is a combination of a rotation about \mathbf{k} and a simultaneous translation along \mathbf{k} which remains unbroken. This leads to a peculiar, strongly anisotropic behavior of the Nambu–Goldstone mode of the broken symmetry [6].

Second, the wavelength of the helical state is proportional to $1/c$, hence the weaker is the DM term, the longer is the scale of the helical ordering. This will be particularly important in the later application to spin-one color superconductivity where the c -term comes from weak interactions and is thus expected to be tiny.

Third, according to Eq. (14), the DM term effectively lowers the coefficient b . Therefore, it leads to a slight increase of the critical temperature, and at a fixed temperature to a slight increase of the magnitude of the magnetization. However, its most notable consequence is the formation of the nonuniform field configuration.

Fourth, as long as we restrict ourselves to terms up to fourth order in Δ in the free energy, the ground state can be rigorously proved to be composed of a single plane wave (and possibly the counterpropagating wave), although the gradient terms are minimized by Fourier modes with momenta lying on a sphere of radius $|\mathbf{k}|_{\min}$.

B. Spin-one color superconductor

The generalization of the GL functional (13) to the case of the spin-one color superconductor is straightforward and unique,

$$\begin{aligned} \mathcal{F}[\vec{\phi}_a] &= a_1 \nabla_i \vec{\phi}_a^\dagger \cdot \nabla_i \vec{\phi}_a + a_2 (\vec{\nabla} \cdot \vec{\phi}_a^\dagger) (\vec{\nabla} \cdot \vec{\phi}_a) \\ &+ b \vec{\phi}_a^\dagger \cdot \vec{\phi}_a + c \vec{\phi}_a^\dagger \cdot (\vec{\nabla} \times \vec{\phi}_a) + d_1 \mathcal{A} + d_2 \mathcal{B} + d_3 \mathcal{C}. \end{aligned} \quad (16)$$

As above, we Fourier-decompose the order parameter field,

$$\vec{\phi}_a(\mathbf{x}) = \sum_{\mathbf{k}} \vec{\varphi}_{a\mathbf{k}} e^{i\mathbf{k}\cdot\mathbf{x}}, \quad (17)$$

and define $\mathcal{M} \equiv \sum_{\mathbf{k}} \vec{\varphi}_{a\mathbf{k}}^\dagger \cdot \vec{\varphi}_{a\mathbf{k}}$. Using the same argument as in the preceding subsection, the free energy is estimated as

$$\frac{1}{\Omega} \int d^3\mathbf{x} \mathcal{F}[\vec{\phi}_a] \geq \left(b - \frac{c^2}{4a_1} \right) \mathcal{M} + \bar{d}\mathcal{M}^2, \quad (18)$$

where the effective quartic coupling \bar{d} for the various spin-one color-superconducting phases was defined in Sec. III A. The absolute minimum of the free energy is achieved for purely transverse configurations with uniform summed magnitude $\vec{\varphi}_a^\dagger \cdot \vec{\varphi}_a$ such that *for all colors* a , the real and imaginary parts of $\vec{\varphi}_{a\mathbf{k}}$ have the same magnitude and together with \mathbf{k} form a left-handed orthogonal system of vectors, and only modes with $|\mathbf{k}| = |\mathbf{k}|_{\min} = c/2a_1$ are included. We shall now construct the helical states for the phases that appear in the phase diagram in Fig. 4.

1. Polar and A phases

A single anticolor participates in the condensation. The ground state can therefore be constructed in complete analogy with Sec. IV A. For the polar phase, the order parameter is real, and we thus find a real standing wave. Choosing the coordinate basis so that the helix points along the z axis, the order parameter takes the form

$$\Delta_{\text{polar}} = \sqrt{\mathcal{A}_{\text{min}}} \begin{pmatrix} 0 & 0 & 0 \\ 0 & 0 & 0 \\ \cos kz & \sin kz & 0 \end{pmatrix}.$$

The condensate magnitude and free energy are given by a modification of Eq. (10),

$$\sqrt{\mathcal{A}_{\text{min}}} = -\frac{b(1+\xi)}{2\bar{d}}, \quad \mathcal{F}_{\text{min}} = -\frac{b^2(1+\xi)^2}{4\bar{d}}, \quad (19)$$

where

$$\xi \equiv -c^2/4a_1b, \quad (20)$$

and as before, $\bar{d}_{\text{polar}} = d_1 + d_2 + d_3$.

In the case of the A phase, the order parameter can also be cast in such a form that only one anticolor condenses. (The matrix Δ is then of course no longer Hermitian.) The nonzero vector $\vec{\phi}_a$ is forced to be “maximally complex” in the sense that $\mathcal{C} = 0$. This leads to the single plane wave solution,

$$\Delta_A = \sqrt{\frac{\mathcal{A}_{\text{min}}}{2}} e^{ikz} \begin{pmatrix} 0 & 0 & 0 \\ 0 & 0 & 0 \\ 1 & -i & 0 \end{pmatrix}.$$

The condensate magnitude and free energy follow from Eq. (19) with $\bar{d}_A = d_1 + d_2$.

2. ε phase

In this phase, the order parameter can be cast in a form that just two anticolors condense, which amounts to adding another orthogonal real vector to the above A -phase order parameter. However, three real vectors cannot be simultaneously orthogonal to each other, and still orthogonal to the momentum \mathbf{k} . This means that the lower bound (18) cannot be reached, or, the gradient and static parts of the free energy cannot be separately minimized for an order parameter of the ε type.

To see what the ground state will look like, we resort to the Ginzburg–Landau equation following from Eq. (16),

$$\begin{aligned} & -a_1 \vec{\nabla}^2 \vec{\phi}_a - a_2 \vec{\nabla} \cdot (\vec{\nabla} \cdot \vec{\phi}_a) + b \vec{\phi}_a + c(\nabla \times \vec{\phi}_a) \\ & + 2d_1 \vec{\phi}_a (\vec{\phi}_b^\dagger \cdot \vec{\phi}_b) + 2d_2 \vec{\phi}_b (\vec{\phi}_a \cdot \vec{\phi}_b^\dagger) + 2d_3 \vec{\phi}_b^\dagger (\vec{\phi}_a \cdot \vec{\phi}_b) = 0. \end{aligned} \quad (21)$$

We are not going to solve this equation directly. After all, even if we did, we could not prove anyway that our solution was the absolute minimum of the free energy. Nonetheless, Eq. (21) will provide us with the necessary insight to make a heuristic guess about the form of the ground state.

The starting assumption is that the values of the order parameter $\vec{\phi}_a$ at different space points are connected by a symmetry transformation. This is reasonable for otherwise the static part of the free energy density would not be uniform; it is hard to imagine how such a configuration could be even a local minimum of the free energy.

The DM term in the “equation of motion” (21) forces the vector $\vec{\phi}_a$ to rotate about the direction of \mathbf{k} . Also, this term does not mix colors. Hence it is plausible that the transformation which connects the values of the order parameter at different points is a pure spatial rotation. Naturally, the axis of rotation is to be identified with the direction of the momentum \mathbf{k} . We can then choose the basis in the color space in such a way that for one anticolor, the vector $\vec{\phi}_a$ is perpendicular to \mathbf{k} and rotates about it (transverse mode), while the vector of the second anticolor is aligned with \mathbf{k} and static (longitudinal mode). This is also in accord with our general discussion since a longitudinal mode with nonzero momentum would cost energy.

With the above argument in mind, we write down the helical state of the ε type with \mathbf{k} along the z axis,

$$\Delta_\varepsilon = \sqrt{\mathcal{A}_{\text{min}}} \begin{pmatrix} 0 & 0 & 0 \\ \sqrt{2}\alpha e^{ikz} & -i\sqrt{2}\alpha e^{ikz} & 0 \\ 0 & 0 & \beta \end{pmatrix} \quad (22)$$

Here k, α, β , and $\sqrt{\mathcal{A}_{\text{min}}}$ are treated as variational parameters with the constraint $4\alpha^2 + \beta^2 = 1$ enforced by normalization. Minimizing the free energy within this class of variational states, we find

$$\begin{aligned} 4\alpha^2 &= \frac{d_2 + d_3 + \xi(d_1 + d_2 + d_3)}{d_2(2 + \xi) + d_3(1 + \xi)}, \\ \beta^2 &= \frac{d_2 - \xi d_1}{d_2(2 + \xi) + d_3(1 + \xi)}, \end{aligned}$$

and the momentum is, as above, given by $k = c/2a_1$. Note that for $\xi = 0$ these expressions reduce to the previous result, Eq. (11). The condensate magnitude and free energy read

$$\begin{aligned} \sqrt{\mathcal{A}_{\text{min}}} &= -\frac{b}{2} \frac{1 + \xi \frac{d_2 + d_3}{2d_2 + d_3}}{d_1 + d_2 \frac{d_2 + d_3}{2d_2 + d_3}}, \\ \mathcal{F}_{\text{min}} &= -\frac{b^2}{4} \frac{1 + 2\xi \frac{d_2 + d_3}{2d_2 + d_3} + \xi^2 \frac{d_1 + d_2 + d_3}{2d_2 + d_3}}{d_1 + d_2 \frac{d_2 + d_3}{2d_2 + d_3}}. \end{aligned}$$

While the denominators of the large fractions contain the expected effective quartic coupling, $\bar{d}_\varepsilon = d_1 + d_2 \frac{d_2 + d_3}{2d_2 + d_3}$, the numerators differ from Eq. (19). This is because the

separate minimization of the gradient and static parts of the free energy could not be achieved so that both the condensate and the condensation energy are actually smaller than Eq. (19) would have predicted.

Apart from the variational minimization of the free energy with the ansatz (22), we also checked explicitly that this state with parameters fixed by the above expressions indeed solves the GL equation (21). This provides a decent evidence that we have found the genuine ground state.

3. CSL phase

Here the situation is even more severe than for the ε phase. In that case, the order parameter contains even after normalization a free parameter, say, the ratio α/β . The effect of the DM term in the free energy is then accounted for by a slight shift of this parameter. However, the CSL order parameter is rigid, there are no free parameters beyond the overall norm to adjust. As a result, the CSL state simply turns out to be incompatible with the DM term: It is no longer a minimum of the free energy.

To see this, let us assume [as in the discussion below Eq. (21)] that the order parameter has everywhere the CSL form with a fixed magnitude. Consequently, the matrix Δ is unitary up to a real coordinate-independent factor. This dramatically simplifies the GL equation (21), which becomes linear and separated for the individual colors,

$$-a_1 \vec{\nabla}^2 \vec{\phi}_a - a_2 \vec{\nabla}(\vec{\nabla} \cdot \vec{\phi}_a) + c \vec{\nabla} \times \vec{\phi}_a + b_{\text{eff}} \vec{\phi}_a = 0,$$

with $b_{\text{eff}} = b + 2\bar{d}_{\text{CSL}}\sqrt{\mathcal{A}}$. Being linear, this equation can be solved independently for the static and rotating modes. In particular the existence of a static mode requires $b_{\text{eff}} = 0$. This fixes the condensate magnitude to its size without the DM term. The rotating mode has to fulfill the condition $a_1|\mathbf{k}|^2 = c|\mathbf{k}|$. Therefore, even though there is a solution with helical structure, its energy is the same as that of the uniform CSL condensate.

In order to resolve this problem, it is important to realize that the anticipated existence of a helical structure in the ground state implies breaking of the rotational symmetry at least to the group of rotations about the axis of the helix, \mathbf{k} . It would be naive to expect the isotropic CSL state in such a situation.

We can take the reduced axial symmetry into account and at the same time relax the rigidity of the order parameter by considering the more general *axial* state (see Fig. 1). This is natural: There is no reason why the static part of the order parameter, aligned with \mathbf{k} , should have the same length as the transverse part, which is perpendicular to \mathbf{k} and rotates about it. In fact, thanks to the DM term, we should expect the transverse part to be

preferred. This argument leads us to the ansatz

$$\Delta_{\text{axial}} = \sqrt{\mathcal{A}_{\text{min}}} \begin{pmatrix} \alpha \cos kz & \alpha \sin kz & 0 \\ -\alpha \sin kz & \alpha \cos kz & 0 \\ 0 & 0 & \beta \end{pmatrix}, \quad (23)$$

with the normalization constraint $2\alpha^2 + \beta^2 = 1$. The variational minimization of the free energy now results in

$$\alpha^2 = \frac{1 + \xi \frac{d_1 + d_2 + d_3}{d_2 + d_3}}{3 + 2\xi}, \quad \beta^2 = \frac{1 - 2\xi \frac{d_1}{d_2 + d_3}}{3 + 2\xi}.$$

The condensate magnitude and free energy are given by

$$\sqrt{\mathcal{A}_{\text{min}}} = -\frac{b}{2} \frac{3 + 2\xi}{3d_1 + d_2 + d_3},$$

$$\mathcal{F}_{\text{min}} = -\frac{b^2}{4} \frac{3 + 4\xi + 2\xi^2 \frac{d_1 + d_2 + d_3}{d_2 + d_3}}{3d_1 + d_2 + d_3}.$$

These results show that α is always larger than β so that the rotating part of the order parameter is indeed favored over the static one, as predicted. In comparison to the CSL state this physically means that one can gain energy by making the condensates of the three anticolors slightly imbalanced in favor of the two anticolors that form the helical structure. This has the amusing consequence that the ground state is no longer color-neutral. The color-density imbalance is a sheer weak-interaction effect.

4. Planar phase

The magnitude β of the static part of the axial order parameter decreases with the sum $d_2 + d_3$ until at $d_2 + d_3 = 2\xi d_1$ it goes to zero. The axial order parameter reduces to the planar one. Since in the phase diagram without the DM term, Fig. 4, the boundary between the CSL and polar phases occurs at $d_2 + d_3 = 0$, we may expect the planar phase to interpose itself between the two at nonzero ξ .

The planar order parameter is explicitly expressed as

$$\Delta_{\text{planar}} = \sqrt{\frac{\mathcal{A}_{\text{min}}}{2}} \begin{pmatrix} \cos kz & \sin kz & 0 \\ -\sin kz & \cos kz & 0 \\ 0 & 0 & 0 \end{pmatrix}, \quad (24)$$

and its size and free energy are given by Eq. (19) with $\bar{d}_{\text{planar}} = d_1 + \frac{d_2 + d_3}{2}$.

C. Phase diagram

The phase diagram, modified by the parity-violating DM term, is displayed in Fig. 5, assuming that $d_1 > 0$. [For $d_1 < 0$, a large part of the (d_2, d_3) plane would be excluded by the requirement of the boundedness of the free energy so that the resulting picture would not be very

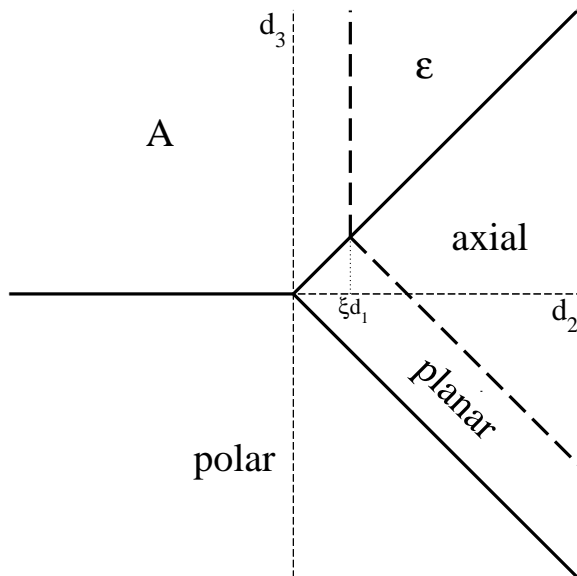


FIG. 5: Phase diagram of the spin-one color superconductor including the DM term. The solid and dashed thick lines denote first- and second-order phase transitions, respectively. The positions of the solid lines are the same as in Fig. 4 and independent of the DM term, whereas the offset of the dashed lines is proportional to the parameter ξ defined in Eq. (20).

interesting.] The ε -A and axial-planar phase transitions are of the second order. They are both characterized by vanishing of the respective β parameter. The rest of the phase transitions are first order.

For the axial and ε states, the minimum free energy suggested by Eq. (18) cannot be achieved. As a result, these two phases are pushed away from the phase diagram by the DM term. The first-order transition lines were determined by a comparison of the free energies of the individual phases. It was thus checked that the free energy is continuous all over the phase diagram, which is a necessary condition for the conclusion that we have not missed any possible intermediate phase and determined the phase diagram correctly.

Finally, note that while the complete GL free energy (16) is $SU(3) \times SO(3) \times U(1)$ -invariant, the DM term has in fact an enhanced $SO(6) \times SO(3)$ symmetry under which the pairs of states A-planar and ε -axial are degenerate. This has in particular the consequence that the ε -axial transition line in the phase diagram (the CSL state being a special case of the axial one) does not shift when the DM term is switched on.

V. MICROSCOPIC DERIVATION OF DM TERM

In this section, we provide a microscopic derivation of the Ginzburg-Landau free energy. Again, a thorough analysis of this problem was performed by Bailin and Love long time ago. Nevertheless, since the calculation

at the level of generality taken up in Ref. [10] is rather involved, we make a number of simplifying assumptions that allow us to arrive at a simple formula in an efficient manner.

A. GL functional from NJL model

First of all, we fix the Dirac structure of the spin-one gap matrix to be simply γ_i . Such an order parameter has positive parity and in the ultrarelativistic limit describes purely transverse pairing of fermions, which was shown in Ref. [19] to be energetically preferred to the longitudinal pairing [52].

Second, we for simplicity disregard the gluonic fluctuations which would otherwise make the superconducting phase transition first order [36], and derive the GL free energy in the framework of the Nambu-Jona-Lasinio (NJL) model [37]. This is decently justified by the fact that the coefficients of the GL free energy are to a large extent universal, the only dynamics-dependent quantity being the critical temperature [10]. The fact that the NJL model does not capture correctly the effects of the soft chromomagnetic gluons and thus predicts wrong asymptotic behavior of the gap and critical temperature, should therefore not matter as long as the critical temperature is appropriately adjusted.

Third, we neglect, as usual, the antiparticle degrees of freedom. As mentioned above, in the ultrarelativistic limit this automatically projects out the transverse part of the order parameter. Here we take the advantage of the fact that the Dirac structure γ_i can be achieved within a NJL-type model with a contact, momentum-independent interaction. Finally, we neglect the admixture of states with higher angular momentum [38, 39].

Given the above assumptions, the mean-field approximation to the NJL model amounts to a theory of noninteracting quasiquarks in the background of the (possibly slowly-varying) order parameter ϕ_{ai} , with the imaginary-time propagator in the Nambu space, $\Psi \equiv (\psi, \psi^c)^T$, given by

$$\mathcal{D}^{-1}(i\omega_n, \mathbf{k}) = \begin{pmatrix} (i\omega_n - \xi_{\mathbf{k}})\gamma_0\Lambda_{\mathbf{k}}^+ & \tilde{\Phi} \\ \Phi & (i\omega_n + \xi_{\mathbf{k}})\gamma_0\Lambda_{\mathbf{k}}^- \end{pmatrix}, \quad (25)$$

where we used the usual notation for $\epsilon_{\mathbf{k}} = \sqrt{\mathbf{k}^2 + m^2}$ and the energy with respect to the Fermi level, $\xi_{\mathbf{k}} = \epsilon_{\mathbf{k}} - \mu$. Also, $\Lambda_{\mathbf{k}}^{\pm} = \frac{1}{2} \left[1 \pm \frac{1}{\epsilon_{\mathbf{k}}} \gamma_0 (\boldsymbol{\gamma} \cdot \mathbf{k} + m) \right]$ are the standard positive/negative energy state projectors, and

$$\Phi = \frac{\lambda_a^A}{\sqrt{2}} \gamma_i \phi_{ai}, \quad \tilde{\Phi} = \gamma_0 \Phi^\dagger \gamma_0, \quad (26)$$

where $(\lambda_a^A)_{bc} = -i\epsilon_{abc}$.

The GL free energy density at weak coupling and in

the ultrarelativistic limit then becomes

$$\mathcal{F}[\vec{\phi}_a] = \frac{7\zeta(3)p_F^3}{240\pi^4\mu T_c^2} \left[2|\nabla_i\vec{\phi}_a|^2 - |\vec{\nabla} \cdot \vec{\phi}_a|^2 \right] + \frac{\mu p_F}{3\pi^2} t |\vec{\phi}_a|^2 + \frac{7\zeta(3)\mu p_F}{480\pi^4 T_c^2} (3\mathcal{A} + 3\mathcal{B} - 2\mathcal{C}), \quad (27)$$

where T_c is the critical temperature for the spin-one pairing. We denoted $t = \frac{T}{T_c} - 1$ and for the sake of an easy check with literature, kept separate symbols for the Fermi momentum p_F and the chemical potential μ , even though they actually coincide in the ultrarelativistic limit. Derivation of the GL functional (27) is routine. Yet we are not aware of any other independent calculation for spin-one color superconductivity using the NJL model, and therefore provide some details in Appendix C.

A comparison with Eq. (5) now yields the phenomenological coefficients

$$a_1 = -2a_2 = \frac{7\zeta(3)p_F^3}{120\pi^4\mu T_c^2}, \quad b = \frac{\mu p_F}{3\pi^2} t, \\ d_1 = d_2 = -\frac{3}{2}d_3 = \frac{7\zeta(3)\mu p_F}{160\pi^4 T_c^2}.$$

The ratio of d_2 and d_3 is indicated in Fig. 4 by a cross. In agreement with the full QCD calculation we conclude that in the absence of the DM term, the weak-coupling limit favors the CSL pattern.

In the presence of the DM term, the form of the ground state depends on the parameter

$$\xi = -\frac{c^2}{4a_1 b} = -c^2 \frac{90\pi^6 T_c^2}{7\zeta(3)p_F^4 t}.$$

As remarked at the end of Sec. IV A, the DM term slightly increases the critical temperature. Eq. (19) suggests that the corrected critical temperature is given by $\xi = -1$ [53], i.e.,

$$t_c = c^2 \frac{90\pi^6 T_c^2}{7\zeta(3)p_F^4}.$$

Just below the (new) critical temperature, ξ is large and negative. With decreasing temperature, it goes through a singularity to large positive values and starts decreasing. (Of course, this “singularity” is completely artificial and comes just from the definition of ξ .) In the tiny window below the critical temperature and above the temperature at which $\xi = 1/6$, the ground state has therefore the planar structure, Eq. (24). Only for $\xi < 1/6$ the system enters the distorted CSL phase—the axial phase, the ground state being as in Eq. (23) with

$$\alpha^2 = \frac{1 + 4\xi}{3 + 2\xi}, \quad \beta^2 = \frac{1 - 6\xi}{3 + 2\xi}.$$

With further decreasing temperature, ξ drops to zero and the ground state relaxes to the CSL state. Needless to say

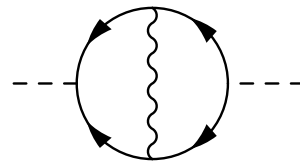


FIG. 6: Pairing field self-energy with Z -boson insertion.

that the temperature range in which this evolution occurs is extremely narrow, but it is nevertheless interesting to observe that the cooling of the system across the critical temperature actually consists of a fast sequence of two phase transitions, both of second order.

B. DM term

The last, and very important, missing ingredient in our analysis is the actual value of the DM coefficient c . We will argue here that the parity-violating DM term is naturally induced by the underlying weak interactions. Since the DM term is bilinear in the order parameter, we will seek weak corrections to the collective pairing mode propagator.

Before we begin the calculation, we make a remark about the discrete symmetries of the DM term. As already stressed, it breaks the parity. At the same time, it is invariant under charge conjugation (up to a total derivative). On the other hand, it is well known that weak interactions in a single-fermion-family world violate parity, but preserve the combined CP transformation. In the vacuum, the DM term would therefore be prohibited, at least as a consequence of weak interactions. However, charge conjugation is broken explicitly by the presence of the dense medium, and the DM term therefore arises from the interplay of weak interactions and many-body physics.

Taking into account Gaussian fluctuations above the mean-field Cooper pair condensate, the pairing field propagator is given by a geometric series of the fermion bubble diagrams [40]. The most straightforward weak correction is then the Z -boson exchange, depicted in Fig. 6. (W^\pm bosons cannot be exchanged since we consider just single-flavor quark matter.) Unfortunately, this does not work for the following reason. As mentioned above, the dominant spin-one pairing pattern in the ultrarelativistic limit is transverse in the relative momentum of the pair. Roughly speaking, it corresponds to pairing with total momentum and orbital momentum zero and total spin one, i.e., opposite helicity (and chirality). The quark interaction vertex with the Z boson can be parameterized as $\gamma^\mu(u + v\gamma_5)$, where

$$u = -\frac{e}{2\sin 2\theta_W} \left(\frac{5}{3} \sin^2 \theta_W - \cos^2 \theta_W \right), \\ v = -\frac{e}{2\sin 2\theta_W},$$

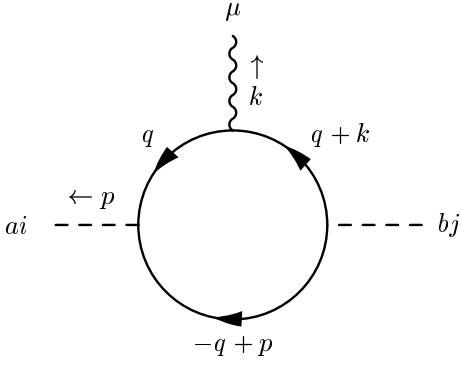


FIG. 7: Effective coupling of the pairing mode to the Z boson. The labels of the fermionic lines denote momentum flowing in the direction of the arrows.



FIG. 8: Pairing field self-energy with Z -boson insertion. The hatched circles denote the effective Z -diquark vertex defined by Fig. 7.

for u -type quarks, and

$$u = \frac{e}{2 \sin 2\theta_W} \left(\frac{1}{3} \sin^2 \theta_W - \cos^2 \theta_W \right),$$

$$v = \frac{e}{2 \sin 2\theta_W},$$

for d -type quarks. Here θ_W is the Weinberg angle and e is the electric charge unit. The coupling of the Z boson to two quarks of opposite chirality in the loop in Fig. 6 then produces the factor $(u+v)(u-v) = u^2 - v^2$. However, to achieve parity breaking, one needs an amplitude odd in v .

We therefore have to look for corrections of higher orders. Since each propagator of a weak intermediate boson is suppressed by the huge weak scale of the order of 100 GeV, it is most likely that any diagram with the exchange of more than one heavy vector boson will be much smaller than a graph with just one Z boson, but including fluctuations of the pairing field. Having in mind that the underlying interaction of the Z boson with the weak neutral quark current induces an effective coupling of Z to the pairing field $\vec{\phi}_a$ (see Fig. 7), we thus anticipate that the leading contribution to the DM term will be given by the graph in Fig. 8. The fact that the diagram involves propagation of an intermediate spin-one collective mode unfortunately means that we will be able to provide only a rough, order-of-magnitude estimate of the DM coefficient c .

We first focus on the effective Z -diquark vertex, $\Gamma_{ai,bj}^\mu(k,p)$, with the vector and axial-vector parts defined by

$$\Gamma_{ai,bj}^\mu(k,p) = uV_{ai,bj}^\mu(k,p) + vA_{ai,bj}^\mu(k,p).$$

For the sake of an analytical estimate of the DM term, we approximate these vertex functions by their Taylor expansion at zero external momentum, working again in the high-density approximation near the Fermi surface [41]. For the vector part of the vertex we thus get

$$V_{ai,bj}^\mu(0,0) = \frac{2\mu}{3\pi^2} \delta^{\mu 0} \delta_{ab} \delta_{ij} \log \frac{2\Lambda_F e^{\gamma-1}}{\pi T_c},$$

where Λ_F is an ultraviolet cutoff on the quark momentum; we will choose it at the order of the Fermi momentum. On the contrary, the axial part of the vertex is finite; it yields the expected parity-violating structure and its Taylor series starts at the first order. Given the $g_{\mu\nu}$ structure of the Z -boson propagator, we just need to evaluate the axial vertex for $\mu = 0$,

$$A_{ai,bj}^0(k,p) = \frac{7i\zeta(3)\mu p_F}{48\pi^4 T_c^2} \delta_{ab} \epsilon_{0ijk} (\mathbf{k} + 2\mathbf{p})_k.$$

The DM term is produced by the diagram in Fig. 8 where one of the effective vertices is vector-like and the other one axial-like. Neglecting the momentum-dependent part of the Z -boson propagator gives

$$\frac{1}{M_Z^2} \not{\int}_k \mathcal{G}_{ck,dl}(k) g_{\mu\nu} \left[A_{ai,ck}^\mu(k-p,p) V_{dl,bj}^\nu(-k+p,k) \right. \\ \left. + V_{ai,ck}^\mu(k-p,p) A_{dl,bj}^\nu(-k+p,k) \right],$$

where we used the shorthand notation for a sum-integral,

$$\not{\int}_k = T \sum_n \int \frac{d^3\mathbf{k}}{(2\pi)^3},$$

and $\mathcal{G}_{ai,bj}$ denotes the collective mode propagator. In the normal phase, it is diagonal in the internal space, $\mathcal{G}_{ai,bj}(k) \equiv \delta_{ab} \delta_{ij} \mathcal{G}(k)$. A comparison with the DM term in Eq. (16) then results in an expression for the coefficient c ,

$$c = \frac{7uv\zeta(3)\mu^2 p_F}{36\pi^6 T_c^2 M_Z^2} \left(\log \frac{2\Lambda_F e^{\gamma-1}}{\pi T_c} \right) \not{\int}_k \mathcal{G}(k).$$

The last sum-integral is apparently quadratically divergent. Part of the divergence comes from the fact that we approximated the effective vertices in Fig. 8 with their low-momentum limits. We therefore make a rough estimate by replacing the Matsubara sums with a frequency integral and putting an ultraviolet cutoff, Λ_B , on the frequency-momentum integration. Taking into account the appropriate volume measure and the fact that the coefficient of the leading, $\mathcal{O}(\mathbf{p}^2)$, in the inverse propagator of the collective mode is typically of order 10^{-1} in the ultrarelativistic limit [42], we find

$$c = \frac{7uv\zeta(3)\mu^2 p_F}{36\pi^6 T_c^2 M_Z^2} \rho, \quad \rho \approx 10^{-1} \Lambda_B^2 \log \frac{2\Lambda_F e^{\gamma-1}}{\pi T_c}. \quad (28)$$

The cutoff Λ_B should be well above the characteristic scale of the pair fluctuations in order not to suppress any physical contribution to the integral; for the moment, we treat it as a free parameter.

VI. PHENOMENOLOGICAL IMPLICATIONS

With all coefficients of the GL functional we can now readily determine the parameters of the ground state. In order to be able to evaluate the condensation energy, we naively extrapolate the GL theory to zero temperature. For a concrete calculation we consider the CSL structure with $\bar{d} = d_1 + \frac{d_2 + d_3}{3}$, in the ultrarelativistic limit where $p_F = \mu$; the orders of magnitude will nevertheless be the same for all phases.

First of all, the wavenumber of the helix in the ground state is given by

$$k_{\text{DM}} = \frac{c}{2a_1} = \frac{5uv\mu\rho}{3\pi^2 M_Z^2}.$$

To appreciate the robustness of the helical ordering, we next compare the condensation energies of the uniform condensation and of the helical ordering itself. The first reads

$$\mathcal{F}_\Delta = -\frac{1}{2}b_0\sqrt{\mathcal{A}} = -\frac{b_0^2}{4d} = -\frac{4\mu^2 T_c^2}{7\zeta(3)},$$

where $b_0 \equiv b/t$, while the latter is

$$\mathcal{F}_{\text{DM}} = -\frac{c^2}{4a_1}\sqrt{\mathcal{A}} = -\frac{5\mu^4}{9\pi^6}\left(\frac{uv\rho}{M_Z^2}\right)^2.$$

[For simplicity, we use the lower bound from Eq. (18) which is not really saturated for the CSL state. However, this only changes the result by a factor of order one.] Apparently, the energy gain from the formation of the helical structure can be many orders of magnitude smaller than the condensation energy of the superconducting state. It is therefore natural to ask whether the long-range helical ordering will not be destroyed by thermal fluctuations of the order parameter.

At low temperatures these will be dominated by the Nambu–Goldstone boson(s) of the spontaneously broken symmetry. The energy density deposited in the thermal fluctuations will therefore be that of the phonon gas with the phase velocity $v_{\text{ph}} = 1/\sqrt{3}$ (in the ultrarelativistic BCS limit), i.e., $3\pi^2 T^4/90v_{\text{ph}}^3$. The helical ordering will be destroyed when this becomes comparable to the condensation energy, \mathcal{F}_{DM} . This leads to the characteristic temperature

$$T_{\text{DM}} \sim \frac{\mu}{\pi^2} \left(\frac{uv\rho}{M_Z^2}\right)^{1/2}.$$

[We dropped the unimportant numerical prefactor $(50/9\sqrt{3})^{1/4}$ which is close to one.]

For temperatures in the range $T_{\text{DM}} \lesssim T \lesssim T_c$, the system will look just like the uniform spin-one color superconductor. Only at temperatures lower than T_{DM} the helical ordering will appear. This change of behavior will, of course, not be associated with any phase transition.

In order to assess the importance of the DM effect, we now make a specific numerical order-of-magnitude estimate. To that end, we need to know that the electroweak couplings are such that $uv \sim 10^{-2}$, the Z -boson mass is of order $M_Z \sim 100$ GeV. We also choose the typical value of the chemical potential to be $\mu = 400$ MeV and set the fermionic cutoff equally, $\Lambda_F = \mu$. There is some controversy in literature regarding the size of the critical temperature, or gap, in spin-one color superconductors. Let us be rather optimistic and assume that $T_c \sim 100$ keV [28]. Using Eq. (28) we thus get

$$\frac{k_{\text{DM}}}{\text{MeV}} \sim 10^{-10} \left(\frac{\Lambda_B}{\text{MeV}}\right)^2, \quad T_{\text{DM}} \sim 10^{-4} \Lambda_B.$$

The choice of the bosonic cutoff Λ_B is obviously crucial. Our rough guess is slightly above the critical temperature itself, $\Lambda_B \sim 1$ MeV. For this value the temperature scale at which the helical ordering takes place becomes 0.1 keV, and the helix wavelength is truly macroscopic—about a millimeter. The temperature scale suggests that the phenomenon could take place in extremely cold quark matter only (six orders of magnitude below the Fermi temperature) such as in very old neutron stars.

In any case, however, the helical ordering in the ground state results in peculiar low-energy properties of the system. As already remarked above, this nonuniform ordering breaks both translational and rotational invariance, leaving unbroken just their special combination. The system will therefore exhibit anisotropic behavior. In helical ferromagnets, the Nambu–Goldstone boson associated with the broken symmetry acts as a magnon when it propagates transversely to the helix axis, and as a phonon when it propagates along [6]. The case of spin-one color superconductors will be similar, in particular we expect that the Nambu–Goldstone mode will have different phase velocities in the transverse and longitudinal directions. This will in turn affect the thermodynamic properties of the system at very low temperatures.

VII. SUMMARY AND DISCUSSION

In this paper we have revised in detail the structure of the ground state of spin-one color superconductors, composed of a single quark flavor. In Sec. II we provided a complete classification of possible ground states distinguished by the unbroken continuous symmetry, assuming a local constant order parameter. In Sec. III we worked out the Ginzburg–Landau description of the spin-one color superconductor near the critical temperature. We wrote down the most general GL free energy up to fourth power in the order parameter and determined its unique global minimum. We thus revealed that the noninert ε state is favored in part of the parameter space.

In Sections IV and V we then argued that the ground state of a spin-one color superconductor will actually be nonuniform as a result of a tiny parity-violating effect

which is due to the electroweak physics. Within the GL analysis, this effect is easily taken into account by adding a new term to the free energy. In analogy with some ferromagnetic materials, the ground state is found to exhibit helical ordering, typically with a wavelength much longer than the characteristic scale of the underlying many-fermion system. This leads in particular to an anisotropic behavior of the system at low temperatures where the helical ordering sets.

In the course of our analysis, we made a number of simplifying assumptions that we wish to discuss to some extent now. First, we assumed that the local structure of the Cooper pair and hence also the classification of Sec. II does not change when the DM term is switched on. This is plausible when the wavelength of the helix is long enough, in particular much longer than the Cooper pair size, so that the spatial modulation of the condensate can be treated as a perturbation. In the realization of the phenomenon considered in this paper, this is guaranteed by the huge ratio of the electroweak vector boson mass to the pairing scale.

Second, while we considered just a positive-parity spin-one condensate, electroweak interactions also induce a small admixture of a negative-parity condensate which makes the GL analysis more involved [10]. This condensate does not interfere with the DM mechanism to the first order in the electroweak effects, and we therefore neglect it here. Moreover, while this condensate would be extremely difficult to detect, the helical ordering of the ground state provides a macroscopic realization of parity violation.

Third, there are other sources of parity violation than direct weak-interaction effects. For instance, condensation of pseudoscalar mesons due to finite chemical potential also breaks parity [43]. However, this is most likely to happen only in the color-flavor-locked phase where all quarks are paired, and hence it is not relevant for spin-one color superconductivity.

Fourth, the fact that the condensate is spatially nonuniform means that the quarks pair with a small, yet nonzero total momentum. In this sense, the helical state is analogous to the Larkin–Ovchinnikov–Fulde–Ferrell state considered in crystalline color superconductors [44, 45]. Different is, of course, the mechanism of the inhomogeneous pairing: In crystalline color superconductors, it is driven by a mismatch of the Fermi surfaces of the quarks to be paired, whereas in the present case the Fermi momenta are exactly equal. The nonzero momentum of the pair is induced by the DM term. The important difference between the various phases considered here is that unlike the real axial, planar, and polar states, the single-plane-wave states A and ε carry nonzero (charge as well as color) current. While in crystalline superconductors this is balanced by a backflow of the unpaired fermions so that the total net current in the ground state is zero [44], the same issue in the A and ε helical phases yet remains to be clarified.

We observe that the axial and planar states which in

a sense interpolate between the CSL and polar phases, show up as physical ground states in the phase diagram. This suggests that they should be seriously taken into consideration even in the absence of the DM term. In particular, in Ref. [29] the effect of color neutrality on spin-one color superconductivity as a complement to the primary 2SC pairing was studied. It was shown that the polar phase may be energetically preferred. Our results open the possibility of an even more favorable state of the axial type, which can compensate the color imbalance of the 2SC pairing and yet gain energy from condensation of all three anticolors.

Finally, we emphasize that the helical ordering by the DM interaction is a fairly general phenomenon; the only two prerequisites are a vector order parameter and broken parity. There are several issues that deserve further investigation. Besides the stress on the spin-one color superconductivity which stems from the pairing of the other quark flavors, we would like to point out in particular the peculiar properties of collective excitations. They will be anisotropic even in the CSL-like axial state and may thus in principle provide a clear manifestation of the nonuniform nature of the ground state. We are going to study these issues in our future work.

Acknowledgments

I am obliged to two people for inspiration which was crucial for this work: to Benedikt Binz, who told me about the fascinating phenomenon of helical ferromagnetism, and to Jiří Hošek, for urging me to look for weak-interaction effects in color superconductors. I am indebted to A. Schmitt for sharing with me his insight in spin-one color superconductivity and for numerous improving remarks and suggestions. I have also benefited from fruitful discussions with H. Abuki, J. Hošek, D. H. Rischke, and Q. Wang. The present research was supported by the Alexander von Humboldt Foundation.

Note added—After this work was completed, I learnt that the same phenomenon was also studied in the context of heavy-fermion superconductors, see [46, 47] and references therein. I thank K. Samokhin for bringing this work to my attention.

APPENDIX A: ORDER PARAMETER

In this appendix we prove Theorems 1 and 2. The basic ingredient will be the polar decomposition, well known from linear algebra.

Theorem 7 (Polar decomposition) *Let M be a square complex matrix. There is a unitary matrix U and a positive-semidefinite Hermitian matrix H such that*

$$M = UH. \quad (A1)$$

The matrix H is unique, while the matrix U is unique if and only if M is nonsingular.

We will not prove this statement here but just remark that when M is singular, the matrix U is determined up to a unitary transformation acting on the eigenvectors of M with zero eigenvalue.

1. Proof of Theorem 1

Thanks to the polar decomposition (A1), we can always make the order parameter Δ Hermitian and positive-semidefinite by a suitable left unitary transformation. We thus have $\Delta = S + iA$, where S (A) is a real (anti)symmetric matrix. As the next and last step we note that a diagonal orthogonal rotation (2) preserves (anti)symmetry, and thus transforms the matrices S, A separately. The real symmetric matrix S can always be diagonalized by such a transformation, which brings the order parameter to the form (3).

2. Proof of Theorem 2

The diagonal orthogonal transformation (2) preserves Hermiticity and the spectrum, hence Eq. (4) says $U\Delta' = \Delta$, where $\Delta' = R^T \Delta R$ and both Δ and Δ' are Hermitian and positive-semidefinite. However, Theorem 7 asserts that the Hermitian part of the polar decomposition is unique. Therefore, we necessarily find $\Delta = \Delta' = R^T \Delta R$ and $U\Delta = \Delta$, as was to be proved.

APPENDIX B: INEQUALITIES BETWEEN QUARTIC INVARIANTS

In this appendix we prove Theorems 3, 4, 5, and 6. Several proofs will be based on the well known Cauchy inequality which asserts that for any two complex vectors u, v , we have

$$\left| \sum_i u_i^* v_i \right|^2 \leq \left(\sum_i |u_i|^2 \right) \left(\sum_i |v_i|^2 \right). \quad (\text{B1})$$

The inequality in Eq. (B1) is saturated if and only if the vectors u, v are collinear.

1. Proof of Theorem 3

Let us denote the (real and positive) eigenvalues of $\Delta\Delta^\dagger$ as δ_i^2 . Then $\mathcal{A} = (\sum_i \delta_i^2)^2$ and $\mathcal{B} = \sum_i \delta_i^4$. The second inequality in Eq. (6) as well as the condition for its saturation follow immediately. For the first inequality, set $u_i = \delta_i^2$ and $v_i = 1$. The Cauchy inequality (B1) then gives $\mathcal{A} \leq 3\mathcal{B}$, as was to be proved. This inequality is saturated when all the eigenvalues δ_i^2 are equal, that is, $\Delta\Delta^\dagger$ is proportional to the unit matrix. The order parameter Δ is then unitary up to a real scale factor and can be brought to the CSL form by a left unitary transformation.

2. Proof of Theorem 4

Using the complex-vector notation, $\mathcal{C} = |\vec{\phi}_a \cdot \vec{\phi}_b|^2$ so that we obviously have $\mathcal{C} \geq 0$ with the equality when all scalar products $\vec{\phi}_a \cdot \vec{\phi}_b$ are zero. Writing $\vec{\phi}_a$ in terms of its real and imaginary parts, this first of all requires $|\text{Re } \vec{\phi}_a| = |\text{Im } \vec{\phi}_a|$ and $\text{Re } \vec{\phi}_a \perp \text{Im } \vec{\phi}_a$ for all rows $\vec{\phi}_a$ of the matrix Δ . One of the vectors, say $\vec{\phi}_1$, can then be cast into a special form by a right orthogonal rotation, so that the order parameter becomes

$$\Delta = \begin{pmatrix} z_1 & iz_1 & 0 \\ z_2 & z_3 & z_4 \\ z_5 & z_6 & z_7 \end{pmatrix}.$$

Let us assume that $z_1 \neq 0$ (if not, we go on processing the second row in the same manner). The orthogonality, $\vec{\phi}_1 \cdot \vec{\phi}_2 = 0$, then implies $z_2 + iz_3 = 0$, and from $\vec{\phi}_2 \cdot \vec{\phi}_2 = 0$, $z_4 = 0$ follows. The vectors $\vec{\phi}_1$ and $\vec{\phi}_2$ are therefore collinear so that $\vec{\phi}_1$ can be made zero by a suitable left unitary transformation. Proceeding in the same manner, we next nullify $\vec{\phi}_2$ and end up with just the third row of Δ , being proportional to $(1, i, 0)$. This is equivalent to the A-phase order parameter.

For the second inequality in Eq. (7), recall that Hermitian matrices span a real vector space with a scalar product defined as $(A, B) = \text{Tr}(AB)$. If we set $Z = \Delta^\dagger \Delta$, we have $\mathcal{B} = \text{Tr}(ZZ) = \|Z\|^2$ and $\mathcal{C} = \text{Tr}(Z^*Z) = (Z^*, Z)$. Therefore, we get

$$0 \leq \|Z - Z^*\|^2 = \|Z\|^2 + \|Z^*\|^2 - 2(Z, Z^*) = 2(\mathcal{B} - \mathcal{C}).$$

We thus prove $\mathcal{C} \leq \mathcal{B}$ with the equality if and only if $Z = Z^*$. This translates into the requirement that $\Delta_{ai}^* \Delta_{aj}$ is real, i.e., all scalar products of columns of Δ must be real. However, the order parameter may always be transformed by a left unitary matrix to the form

$$\Delta = \begin{pmatrix} a_1 & z_1 & z_2 \\ 0 & a_2 & z_3 \\ 0 & 0 & a_3 \end{pmatrix},$$

with real a_i and complex z_i . Applying step by step the above reality requirement we find that the whole matrix actually has to be real.

3. Proof of Theorem 5

As already mentioned in Appendix B2, we can define a scalar product of two Hermitian matrices by the trace of their matrix product. We now introduce some further notation. We first define an orthonormal basis, $T_a, a = 0, \dots, 8$, so that $(T_a, T_b) = \delta_{ab}$. These matrices are simply defined as $T_0 = \mathbb{1}/\sqrt{3}$ and $T_a = \lambda_a/\sqrt{2}, a = 1, \dots, 8$, in terms of the standard Gell-Mann matrices. Expanding a given Hermitian matrix in this basis, e.g. $A = a_a T_a$, the scalar product becomes $(A, B) = a_a b_a$.

As above we denote $Z = \Delta^\dagger \Delta$. Recalling that the basis matrices T_2, T_5, T_7 are imaginary while all others are real, we can see that the complex conjugation in Z^* just changes the sign of the coordinates z_2, z_5, z_7 . Introducing finally the shorthand notation,

$$\begin{aligned} u^2 &= z_0^2, & w^2 &= z_2^2 + z_5^2 + z_7^2, \\ v^2 &= z_1^2 + z_3^2 + z_4^2 + z_6^2 + z_8^2, \end{aligned} \quad (\text{B2})$$

we obtain the expressions for the three invariants,

$$\begin{aligned} \mathcal{A} &= (\text{Tr } Z)^2 = (Z, \mathbb{1})^2 = 3u^2, \\ \mathcal{B} &= (Z, Z) = u^2 + v^2 + w^2, \\ \mathcal{C} &= (Z^*, Z) = u^2 + v^2 - w^2. \end{aligned}$$

This implies $\mathcal{B} + \mathcal{C} = 2(u^2 + v^2)$, whence we immediately get the desired inequality (8). It will be saturated if and only if $v = 0$, i.e., if the real part of $Z \equiv \Delta^\dagger \Delta$ will be proportional to the unit matrix. After substitution for the order parameter from (3), it is straightforward to show that this is equivalent to the condition stated in Theorem 5.

4. Proof of Theorem 6

This inequality is most tricky because it does not hold for all matrices Δ but just for those satisfying $\mathcal{C} \leq \frac{1}{9}\mathcal{A}$. We will need another auxiliary claim.

Theorem 8 *Every Hermitian positive-semidefinite matrix Z satisfies the following inequality,*

$$v \geq w\sqrt{3} - u\sqrt{2}, \quad (\text{B3})$$

where the non-negative quantities u, v, w are defined by Eq. (B2). The inequality is saturated if and only if Z is of the ε type.

Proof.—By a suitable diagonal orthogonal rotation, $Z \rightarrow R^T Z R$, we can always make the coordinates z_5 and z_7 vanish so that $z_2 = \pm w$. Let us without lack of generality assume that $z_2 = w$. Pick up a test vector as the eigenvector of λ_2 with the eigenvalue -1 , $|t\rangle = \frac{1}{\sqrt{2}}(1, -i, 0)^T$. The expectation value of Z is

$$\langle t|Z|t\rangle = \frac{u}{\sqrt{3}} + \frac{z_8}{\sqrt{6}} - \frac{w}{\sqrt{2}}.$$

Positive-semidefiniteness requires that this be non-negative, which leads to

$$w\sqrt{3} \leq z_8 + u\sqrt{2} \leq v + u\sqrt{2}.$$

The inequality (B3) is thus proved. In order for it to be saturated, we must have $v = z_8$, i.e., $z_1 = z_3 = z_4 = z_6 = 0$, and $z_8 = w\sqrt{3} - u\sqrt{2}$. The matrix Z then reads $Z = \frac{u}{\sqrt{3}}\mathbb{1} + \frac{w}{\sqrt{2}}\lambda_2 + \frac{1}{\sqrt{2}}(w\sqrt{3} - u\sqrt{2})\lambda_8$, which has the ε form with $\Delta_1 = w/\sqrt{2}$ and $\Delta_2 = u\sqrt{3} - w\sqrt{2}$.

We now get to the proof of Theorem 6. For $\mathcal{C} \leq \frac{1}{9}\mathcal{A}$ we find using Theorem 5,

$$\mathcal{B} - \mathcal{C} \geq \frac{2}{3}\mathcal{A} - 2\mathcal{C} \geq \frac{2}{3}\mathcal{A} - \frac{2}{9}\mathcal{A} = \frac{4}{9}\mathcal{A},$$

whence $\frac{2}{\sqrt{3}}u = \frac{2}{3}\sqrt{\mathcal{A}} \leq \sqrt{\mathcal{B} - \mathcal{C}} = w\sqrt{2}$. This means that the right-hand side of the inequality (B3) is non-negative, and the inequality can be equivalently squared. This yields

$$\begin{aligned} v^2 &\geq (w\sqrt{3} - u\sqrt{2})^2 = 3w^2 - 2\sqrt{6}uw + 2u^2, \\ \mathcal{C} = u^2 + v^2 - w^2 &\geq 2w^2 - 2\sqrt{6}uw + 3u^2 = (w\sqrt{2} - u\sqrt{3})^2, \\ \sqrt{\mathcal{C}} &\geq u\sqrt{3} - w\sqrt{2} = \sqrt{\mathcal{A}} - \sqrt{\mathcal{B} - \mathcal{C}}. \end{aligned}$$

The saturation condition is the same as that for the inequality (B3). Since the order parameter Δ is Hermitian and positive-semidefinite without lack of generality, it is given by the unique square root of $Z = \Delta^\dagger \Delta$. It is therefore ε -like if and only if Z is ε -like.

APPENDIX C: GL FREE ENERGY FROM NJL MODEL

In the NJL model, the mean-field free energy of a superconductor is determined by the quasifermionic excitations above the Fermi sea, and is given in terms of the fermion propagator (25) as

$$\mathcal{F} = -\frac{T}{2\Omega} \text{Tr} \log \mathcal{D}^{-1}.$$

Here the trace is taken in the functional sense and the factor $\frac{1}{2}$ comes from doubling of the number of degrees of freedom in the Nambu formalism. The condensate contribution, quadratic in the order parameter, is not included here for it essentially only serves to adjust the GL coefficient b to zero at the critical temperature. Writing the inverse propagator as usual as $\mathcal{D}^{-1} = \mathcal{D}_0^{-1} + \Sigma$, where the self-energy Σ is off-diagonal in the Nambu space and contains the pairing field, expanding in powers of the order parameter up to fourth order, and subtracting the free energy of the normal phase, the GL functional becomes

$$\mathcal{F} = \frac{T}{2\Omega} \left[\frac{1}{2} \text{Tr}(\mathcal{D}_0 \Sigma)^2 + \frac{1}{4} \text{Tr}(\mathcal{D}_0 \Sigma)^4 \right].$$

The traces here lead to momentum integrals which are evaluated in the high-density approximation [41]: The integral over the momentum magnitude, $|\mathbf{k}|$, is replaced with one over the energy measured with respect to the Fermi sea, $\xi_{\mathbf{k}}$, multiplied by the density of states at the Fermi surface, $\mathcal{N} = \frac{\mu p_F}{2\pi^2}$.

Assuming for a moment the generic form of the gap matrix, $\Phi(x) = \phi_a(x)T_a$, where T_a is a set of momentum-independent matrices in the Dirac and fermion-species (flavor) space, the individual terms (referred to as the

“gradient”, “mass”, and “quartic” terms with obvious meaning) in the GL free energy density become

$$\begin{aligned} \text{gradient term} &= \frac{7\zeta(3)p_F^3}{32\pi^2\mu^2T_c^2} \mathcal{N} \sum_{\mathbf{q}} \mathbf{q}^2 \varphi_{a,\mathbf{q}}^* \varphi_{b,-\mathbf{q}} \\ &\quad \times \langle (\hat{\mathbf{p}} \cdot \hat{\mathbf{q}})^2 \text{Tr}(\Lambda_{\mathbf{p}}^+ T_a^\dagger \Lambda_{-\mathbf{p}}^- T_b) \rangle_{\mathbf{p}}, \end{aligned}$$

$$\text{mass term} = \frac{1}{2} \mathcal{N} t \phi_a^* \phi_b \langle \text{Tr}(\Lambda_{\mathbf{p}}^+ T_a^\dagger \Lambda_{-\mathbf{p}}^- T_b) \rangle_{\mathbf{p}},$$

$$\begin{aligned} \text{quartic term} &= \frac{7\zeta(3)}{32\pi^2T_c^2} \mathcal{N} \phi_a^* \phi_b \phi_c^* \phi_d \\ &\quad \times \langle \text{Tr}(\Lambda_{\mathbf{p}}^+ T_a^\dagger \Lambda_{-\mathbf{p}}^- T_b \Lambda_{\mathbf{p}}^+ T_c^\dagger \Lambda_{-\mathbf{p}}^- T_d) \rangle_{\mathbf{p}}. \end{aligned}$$

In all the expressions, angular brackets denote averaging over directions of the indicated momentum, and the hats unit vectors. Also, $\varphi_{a,\mathbf{q}}$ are the Fourier components of the order parameter, defined as in Eq. (17), and the traces are now taken in the Dirac and flavor space. The above expressions are valid for zero as well as finite fermion mass and it is understood that in the projectors $\Lambda_{\pm\mathbf{p}}$ the energy $\epsilon_{\mathbf{p}}$ and momentum \mathbf{p} are replaced with their values on the Fermi level, i.e., μ and $p_F \hat{\mathbf{p}}$.

One can readily check the validity of the general result above on a particularly simple example, namely the (relativistic) BCS superconductor. Here we have just a single order parameter, ϕ , and the corresponding matrix $T = \gamma_5$, which ensures positive-parity pairing. All the Dirac traces are then equal to two and the only nontrivial angular average is $\langle (\hat{\mathbf{p}} \cdot \hat{\mathbf{q}})^2 \rangle_{\mathbf{p}} = \frac{1}{3}$, so that we recover the well-known GL functional of the BCS theory [10],

$$\mathcal{F}_{\text{BCS}} = \frac{7\zeta(3)p_F^3}{96\pi^4\mu T_c^2} |\vec{\nabla}\phi|^2 + \frac{\mu p_F}{2\pi^2} t |\phi|^2 + \frac{7\zeta(3)\mu p_F}{32\pi^4 T_c^2} |\phi|^4.$$

1. GL functional for spin-one color superconductors

The calculation of the GL coefficients may be pushed forward by making a particular assumption on the structure of the gap matrix. It is instructive to divide the calculation in two steps and assume first the spin-one pairing structure $\Phi = \phi_{ai} Q_a \gamma_i$, where the Q_a 's are yet unspecified matrices in the flavor space, normalized for the sake of convenience by $\text{Tr}_F(Q_a Q_b^\dagger) = \delta_{ab}$. The bilinear terms in the GL free energy are then straightforward to evaluate using the explicit form of the energy projectors,

$$\begin{aligned} [\gamma]: \quad \text{gradient term} &= \frac{7\zeta(3)p_F^3}{96\pi^4\mu T_c^2} \\ &\quad \times \left[\left(1 - \frac{p_F^2}{5\mu^2}\right) |\nabla_i \vec{\phi}_a|^2 - \frac{2p_F^2}{5\mu^2} |\vec{\nabla} \cdot \vec{\phi}_a|^2 \right], \quad (\text{C1}) \end{aligned}$$

$$[\gamma]: \quad \text{mass term} = \frac{\mu p_F}{2\pi^2} \left(1 - \frac{p_F^2}{3\mu^2}\right) t |\vec{\phi}_a|^2. \quad (\text{C2})$$

To calculate the Dirac trace in the quartic term, we resort to the ultrarelativistic limit. In this case, the energy projectors reduce the spatial γ -matrices to their transverse parts,

$$\gamma_{\perp i} = \mathcal{P}_{ij} \gamma_j, \quad \mathcal{P}_{ij} = \delta_{ij} - \hat{p}_i \hat{p}_j,$$

and the Dirac trace simplifies to

$$\frac{1}{2} \text{Tr}_D(\gamma_{\perp i} \gamma_{\perp j} \gamma_{\perp k} \gamma_{\perp l}) = 2(\mathcal{P}_{ij} \mathcal{P}_{kl} - \mathcal{P}_{ik} \mathcal{P}_{jl} + \mathcal{P}_{il} \mathcal{P}_{jk}).$$

Using the identity

$$\langle \mathcal{P}_{ij} \mathcal{P}_{kl} \rangle_{\mathbf{p}} = \frac{1}{15} (6\delta_{ij} \delta_{kl} + \delta_{ik} \delta_{jl} + \delta_{il} \delta_{jk}),$$

we finally get

$$\begin{aligned} [\gamma]: \quad \text{quartic term} &= \frac{7\zeta(3)\mu p_F}{240\pi^4 T_c^2} (3\delta_{ij} \delta_{kl} - 2\delta_{ik} \delta_{jl} + 3\delta_{il} \delta_{jk}) \\ &\quad \times \phi_{ai}^* \phi_{bj} \phi_{ck}^* \phi_{dl} \text{Tr}_F(Q_a^\dagger Q_b Q_c^\dagger Q_d). \quad (\text{C3}) \end{aligned}$$

Eqs. (C1), (C2), and (C3) summarize the general Ginzburg–Landau functional for a pairing with the Dirac structure γ_i . In particular for the spin-one pairing considered in this paper, the gap matrix has the form (26). The flavor trace is then $\text{Tr}_F(Q_a^\dagger Q_b Q_c^\dagger Q_d) = \frac{1}{4}(\delta_{ab} \delta_{cd} + \delta_{ad} \delta_{bc})$. Putting all the pieces together, we arrive at the expression for the free energy in Eq. (27).

While the transverse pairing can be achieved with the Dirac structure γ_i , setting $\Phi = \phi_{ai} Q_a \gamma_0 \gamma_i$ leads (in the ultrarelativistic limit) to a purely longitudinal pairing. In this case, the Dirac traces become trivial and we just quote the final result,

$$\begin{aligned} [\gamma_0 \gamma]: \quad \text{gradient term} &= \frac{7\zeta(3)p_F^3}{96\pi^4\mu T_c^2} \\ &\quad \times \left[\left(1 - \frac{4p_F^2}{5\mu^2}\right) |\nabla_i \vec{\phi}_a|^2 + \frac{2p_F^2}{5\mu^2} |\vec{\nabla} \cdot \vec{\phi}_a|^2 \right], \quad (\text{C4}) \end{aligned}$$

$$[\gamma_0 \gamma]: \quad \text{mass term} = \frac{\mu p_F}{2\pi^2} \left(1 - \frac{2p_F^2}{3\mu^2}\right) t |\vec{\phi}_a|^2. \quad (\text{C5})$$

$$\begin{aligned} [\gamma_0 \gamma]: \quad \text{quartic term} &= \frac{7\zeta(3)\mu p_F}{480\pi^4 T_c^2} (\delta_{ij} \delta_{kl} + \delta_{ik} \delta_{jl} + \delta_{il} \delta_{jk}) \\ &\quad \times \phi_{ai}^* \phi_{bj} \phi_{ck}^* \phi_{dl} \text{Tr}_F(Q_a^\dagger Q_b Q_c^\dagger Q_d). \quad (\text{C6}) \end{aligned}$$

As in the previous case, Eqs. (C4) and (C5) are valid for arbitrary fermion mass, while the quartic term (C6) was for simplicity derived in the ultrarelativistic limit.

In the end we would like to remark that a simple special case of our GL functional for spin-one color superconductors is the pairing of quarks of a single color and

two flavors in the antisymmetric flavor-singlet channel, studied by Buballa *et al.* [14]. In this case, the flavor matrix is given by $Q = \frac{1}{\sqrt{2}}\tau_2 \otimes \mathcal{P}_3^{(c)}$, where τ_2 is the Pauli matrix in flavor space and $\mathcal{P}_3^{(c)}$ the projector on the third quark color. The order parameter is a complex vector, $\vec{\phi}$, and one immediately finds, in the ultrarelativistic limit,

$$\mathcal{F}_\gamma = \frac{7\zeta(3)p_F^3}{240\pi^4\mu T_c^2} \left[2|\nabla_i\vec{\phi}|^2 - |\vec{\nabla} \cdot \vec{\phi}|^2 \right] + \frac{\mu p_F}{3\pi^2} t|\vec{\phi}|^2 + \frac{7\zeta(3)\mu p_F}{240\pi^4 T_c^2} \left[3(\vec{\phi}^\dagger \cdot \vec{\phi})^2 - |\vec{\phi} \cdot \vec{\phi}|^2 \right],$$

$$\mathcal{F}_{\gamma_0\gamma} = \frac{7\zeta(3)p_F^3}{480\pi^4\mu T_c^2} \left[|\nabla_i\vec{\phi}|^2 + 2|\vec{\nabla} \cdot \vec{\phi}|^2 \right] + \frac{\mu p_F}{6\pi^2} t|\vec{\phi}|^2 + \frac{7\zeta(3)\mu p_F}{960\pi^4 T_c^2} \left[2(\vec{\phi}^\dagger \cdot \vec{\phi})^2 + |\vec{\phi} \cdot \vec{\phi}|^2 \right].$$

It is amusing to observe that the transverse and longitudinal cases differ in the sign of the $|\vec{\phi} \cdot \vec{\phi}|^2$ term, which results in qualitatively different forms of the ground state. In the γ case the negative sign leads to a polar-like state, $\vec{\phi} \sim (0, 0, 1)^T$. On the other hand, the positive sign in the $\gamma_0\gamma$ case (actually considered in [14]) leads to an A-like state, $\vec{\phi} \sim (1, i, 0)^T$, with peculiar properties such as the existence of a single Nambu–Goldstone boson with a quadratic dispersion relation—the spin wave [14, 35].

-
- [1] I. Dzyaloshinsky, *J. Phys. Chem. Solids* **4**, 241 (1958).
[2] T. Moriya, *Phys. Rev.* **120**, 91 (1960).
[3] B. I. Shraiman and E. D. Siggia, *Phys. Rev. Lett.* **62**, 1564 (1989).
[4] P. Bak and M. H. Jensen, *J. Phys.* **C13**, L881 (1980).
[5] O. Nakanishi, A. Yanase, A. Hasegawa, and M. Kataoka, *Solid State Commun.* **35**, 995 (1980).
[6] T. R. Kirkpatrick and D. Belitz, *Phys. Rev.* **B72**, 180402 (2005).
[7] B. Binz, A. Vishwanath, and V. Aji, *Phys. Rev. Lett.* **96**, 207202 (2006).
[8] B. Binz and A. Vishwanath, *Phys. Rev.* **B74**, 214408 (2006).
[9] M. G. Alford, A. Schmitt, K. Rajagopal, and T. Schaefer (2007), arXiv:0709.4635 [hep-ph].
[10] D. Bailin and A. Love, *Phys. Rept.* **107**, 325 (1984).
[11] T. Schaefer, *Phys. Rev.* **D62**, 094007 (2000), hep-ph/0006034.
[12] J. Hošek (2000), hep-ph/0011034.
[13] M. G. Alford, J. A. Bowers, J. M. Cheyne, and G. A. Cowan, *Phys. Rev.* **D67**, 054018 (2003), hep-ph/0210106.
[14] M. Buballa, J. Hošek, and M. Oertel, *Phys. Rev. Lett.* **90**, 182002 (2003), hep-ph/0204275.
[15] A. Schmitt, Q. Wang, and D. H. Rischke, *Phys. Rev.* **D66**, 114010 (2002), nucl-th/0209050.
[16] A. Schmitt, Q. Wang, and D. H. Rischke, *Phys. Rev. Lett.* **91**, 242301 (2003), nucl-th/0301090.
[17] A. Schmitt, Q. Wang, and D. H. Rischke, *Phys. Rev.* **D69**, 094017 (2004), nucl-th/0311006.
[18] A. Schmitt (2004), nucl-th/0405076.
[19] A. Schmitt, *Phys. Rev.* **D71**, 054016 (2005), nucl-th/0412033.
[20] D. N. Aguilera, D. Blaschke, M. Buballa, and V. L. Yudichev, *Phys. Rev.* **D72**, 034008 (2005), hep-ph/0503288.
[21] D. N. Aguilera, D. Blaschke, H. Grigorian, and N. N. Scoccola, *Phys. Rev.* **D74**, 114005 (2006), hep-ph/0604196.
[22] D. N. Aguilera, *Astrophys. Space Sci.* **308**, 443 (2007), hep-ph/0608041.
[23] A. Schmitt, I. A. Shovkovy, and Q. Wang, *Phys. Rev. Lett.* **94**, 211101 (2005), hep-ph/0502166.
[24] A. Schmitt, I. A. Shovkovy, and Q. Wang, *Phys. Rev. Lett.* **95**, 159902(E) (2005).
[25] A. Schmitt, I. A. Shovkovy, and Q. Wang, *Phys. Rev.* **D73**, 034012 (2006), hep-ph/0510347.
[26] B. A. Sa'd, I. A. Shovkovy, and D. H. Rischke, *Phys. Rev.* **D75**, 065016 (2007), astro-ph/0607643.
[27] D. Blaschke, F. Sandin, T. Klahn, and J. Berdermann (2008), arXiv:0807.0414 [nucl-th].
[28] F. Marhauser, D. Nickel, M. Buballa, and J. Wambach, *Phys. Rev.* **D75**, 054022 (2007), hep-ph/0612027.
[29] M. G. Alford and G. A. Cowan, *J. Phys.* **G32**, 511 (2006), hep-ph/0512104.
[30] D. Vollhardt and P. Wölfle, *The Superfluid Phases of Helium 3* (Taylor and Francis, 1990).
[31] G. Barton and M. A. Moore, *J. Phys.* **C7**, 4220 (1974).
[32] K. Iida and G. Baym, *Phys. Rev.* **D63**, 074018 (2001), hep-ph/0011229.
[33] J. Kim, *Nucl. Phys.* **B196**, 285 (1982).
[34] S. C. Frautschi and J. Kim, *Nucl. Phys.* **B196**, 301 (1982).
[35] T. Brauner, *Phys. Rev.* **D72**, 076002 (2005), hep-ph/0508011.
[36] J. L. Noronha, H.-c. Ren, I. Giannakis, D. Hou, and D. H. Rischke, *Phys. Rev.* **D73**, 094009 (2006), hep-ph/0602218.
[37] M. Buballa, *Phys. Rept.* **407**, 205 (2005), hep-ph/0402234.
[38] B. Feng, D.-f. Hou, and H.-c. Ren, *Nucl. Phys.* **B796**, 500 (2008), arXiv:0711.0496 [hep-ph].
[39] B. Feng, D.-f. Hou, and H.-c. Ren (2008), arXiv:0810.3142 [hep-ph].
[40] H. Abuki, *Nucl. Phys.* **A791**, 117 (2007), hep-ph/0605081.
[41] G. Nardulli, *Riv. Nuovo Cim.* **25N3**, 1 (2002), hep-

- ph/0202037.
- [42] T. Brauner, Phys. Rev. **D77**, 096006 (2008), arXiv:0803.2422 [hep-ph].
- [43] A. Kryjevski, D. B. Kaplan, and T. Schafer, Phys. Rev. **D71**, 034004 (2005), hep-ph/0404290.
- [44] M. G. Alford, J. A. Bowers, and K. Rajagopal, Phys. Rev. **D63**, 074016 (2001), hep-ph/0008208.
- [45] R. Casalbuoni and G. Nardulli, Rev. Mod. Phys. **76**, 263 (2004), hep-ph/0305069.
- [46] V. P. Mineev and K. V. Samokhin, JETP **78**, 401 (1994).
- [47] V. P. Mineev and K. V. Samokhin, Phys. Rev. **B78**, 144503 (2008).
- [48] R. D. Pisarski and D. H. Rischke, Phys. Rev. **D61**, 074017 (2000), nucl-th/9910056.
- [49] Note that in condensed-matter physics, the term “axial” is sometimes used to refer to the A phase [31]. In the context of the spin-one color superconductivity, the term A phase is used exclusively so that no confusion can arise.
- [50] In a ferromagnet the order parameter \vec{M} would, of course, be real. Also, the a_2 term would be absent owing to the fact that there are no magnetic charges. This slight generalization of the GL functional of Ref. [8] allows us to work out an analysis which will later apply almost without change to spin-one color superconductivity.
- [51] While in ordinary ferromagnets, SO(3) rotational invariance is broken down to SO(2) rotations about the direction of the magnetization, here the rotational invariance is broken completely, thanks to the presence of another vector, \mathbf{k} . The group of translations along \mathbf{k} is broken down to its discrete subgroup, defined by the wavelength of the helix. Note that this still allows quasiparticle low-energy excitations with a well defined momentum.
- [52] We stress that the terms transverse and longitudinal here, commonly used in literature [19, 48], have different meaning than those used in Sec. IV. Briefly, in case of fermion pairing, the terms transverse/longitudinal correspond to the *relative*-momentum structure of the Cooper pair, while in case of the (vector) order parameter, they refer to its dependence on the *total* momentum of the Cooper pair. We believe that no confusion can arise.
- [53] In fact, this quantitative estimate of the shift of the critical temperature should not be really trusted, for in our derivation of the DM coefficient c , we neglect analogous weak-interaction contributions to b itself. However, the following qualitative conclusions about the evolution of the ground state just below the critical temperature remain valid.